Electronic Supplementary Information

DNA and BSA Binding, Anticancer and Antimicrobial Properties of Co(II), Co(II/III), Cu(II) and Ag(I) Complexes of Arylhydrazones of Barbituric Acid

Jessica Palmucci,[a,b] Kamran T. Mahmudov,[a,c,*] M. Fátima C. Guedes da Silva,[a,*]
Fabio Marchetti,[b] Claudio Pettinari,[d] Dezemona Petrelli,[e] Luca A. Vitali,[f] Luana Quassinti,[f]
Massimo Bramucci,[d] Giulio Lupidi,[f,*] Armando J. L. Pombeiro[a,*]

[a] Centro de Química Estrutural, Instituto Superior Técnico, Universidade de Lisboa, Av. Rovisco Pais, 1049–001 Lisbon, Portugal
[b] School of Science and Technology, University of Camerino, Chemistry Section, via S. Agostino 1, 62032 Camerino, Italy
[c] Department of Chemistry, Baku State University, Z. Xalilov Str. 23, Az 1148 Baku, Azerbaijan
[d] School of Pharmacy, University of Camerino, Chemistry Section, via S. Agostino 1, 62032 Camerino, Italy
[e] School of Biosciences and Veterinary Medicine, University of Camerino, Piazza dei Costanti 4, 62032 Camerino, Italy
[f] School of Pharmacy, University of Camerino, Biological Section, via Gentile III da Varano, 62032 Camerino, Italy

[*]Corresponding authors
E-mail addresses:
kamran_chem@mail.ru, kamran_chem@yahoo.com (Kamran T. Mahmudov)
fatima.guedes@tecnico.ulisboa.pt (M. Fátima C. Guedes da Silva)
giulio.lupidi@unicam.it (Giulio Lupidi)
pombeiro@tecnico.ulisboa.pt (Armando J. L. Pombeiro)

1. Synthesis of 2

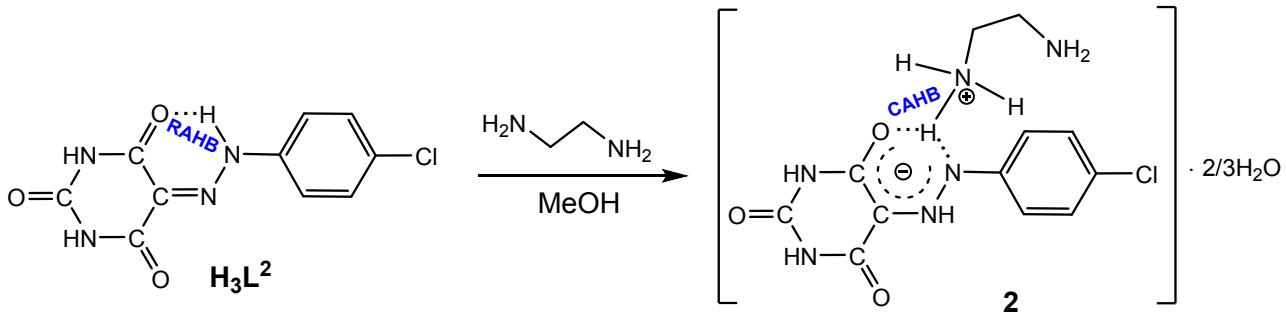

Scheme 1S. RAHB to CAHB transformations in the synthesis of **2**.

2. NMR and IR spectra of H_3L^2, 1, 2, 7 and 8.

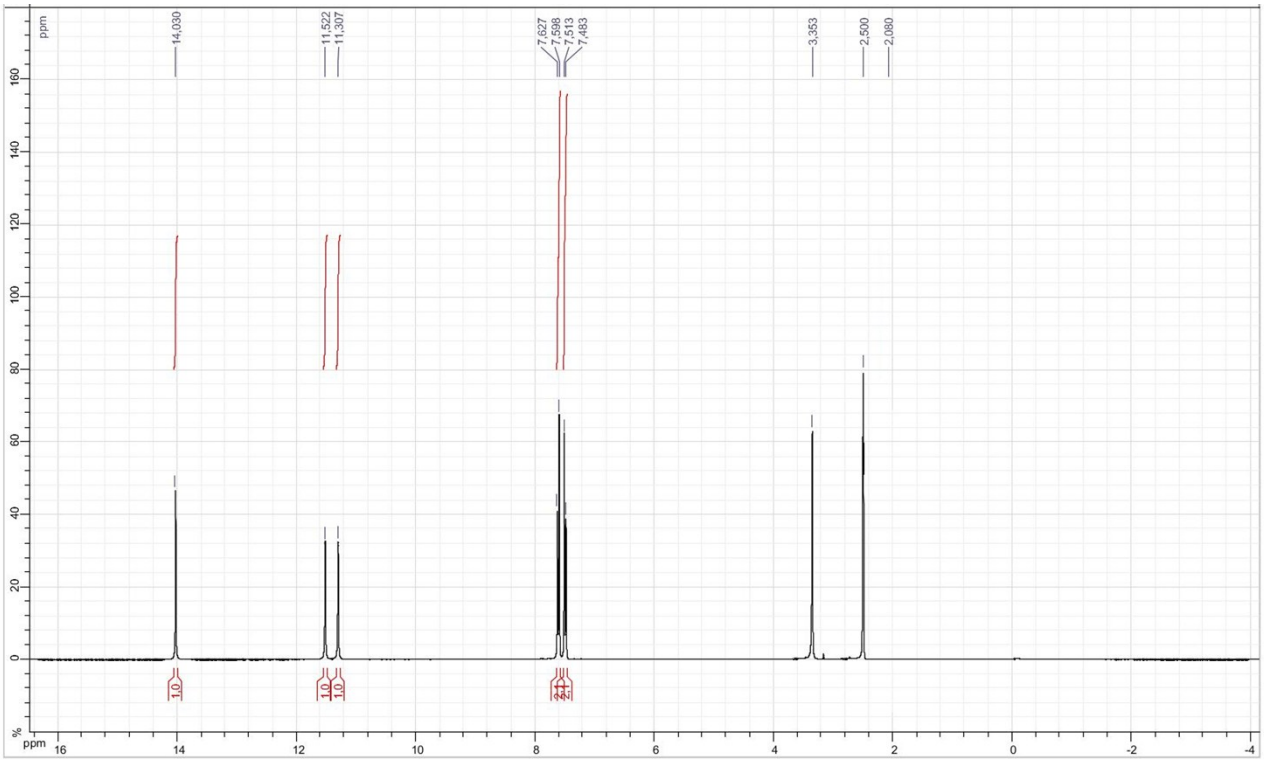

Figure 1S. ^{1}H NMR spectra of **H_3L^2**.

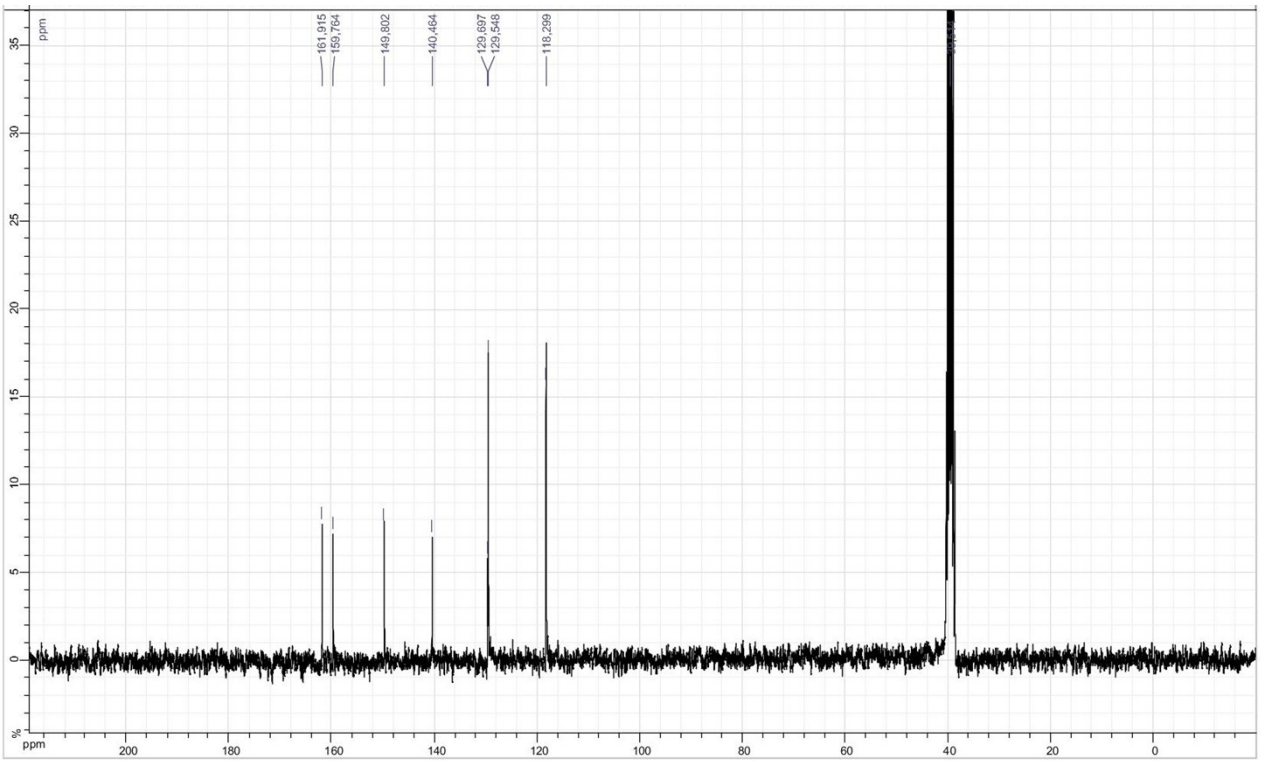

Figure 2S. ^{13}C NMR spectra of $\mathbf{H_3L^2}$.

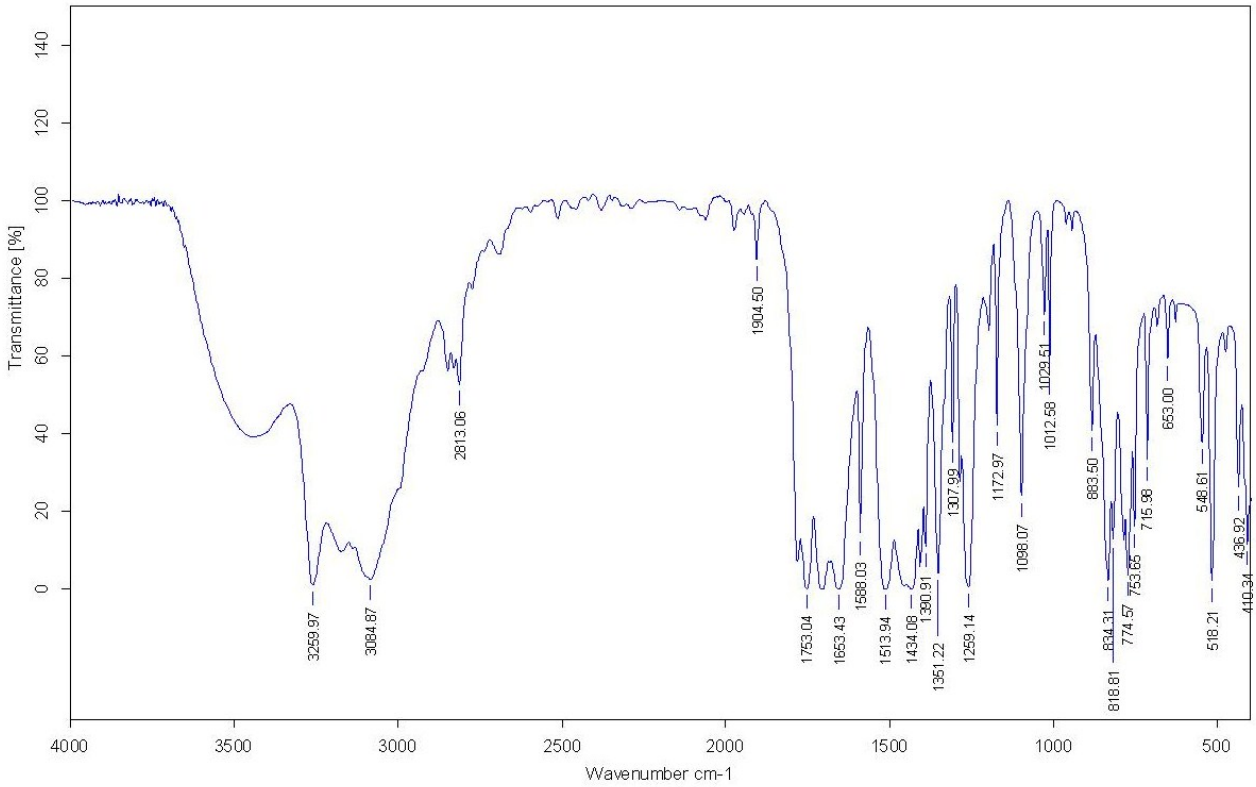

Figure 3S. IR spectra of $\mathbf{H_3L^2}$.

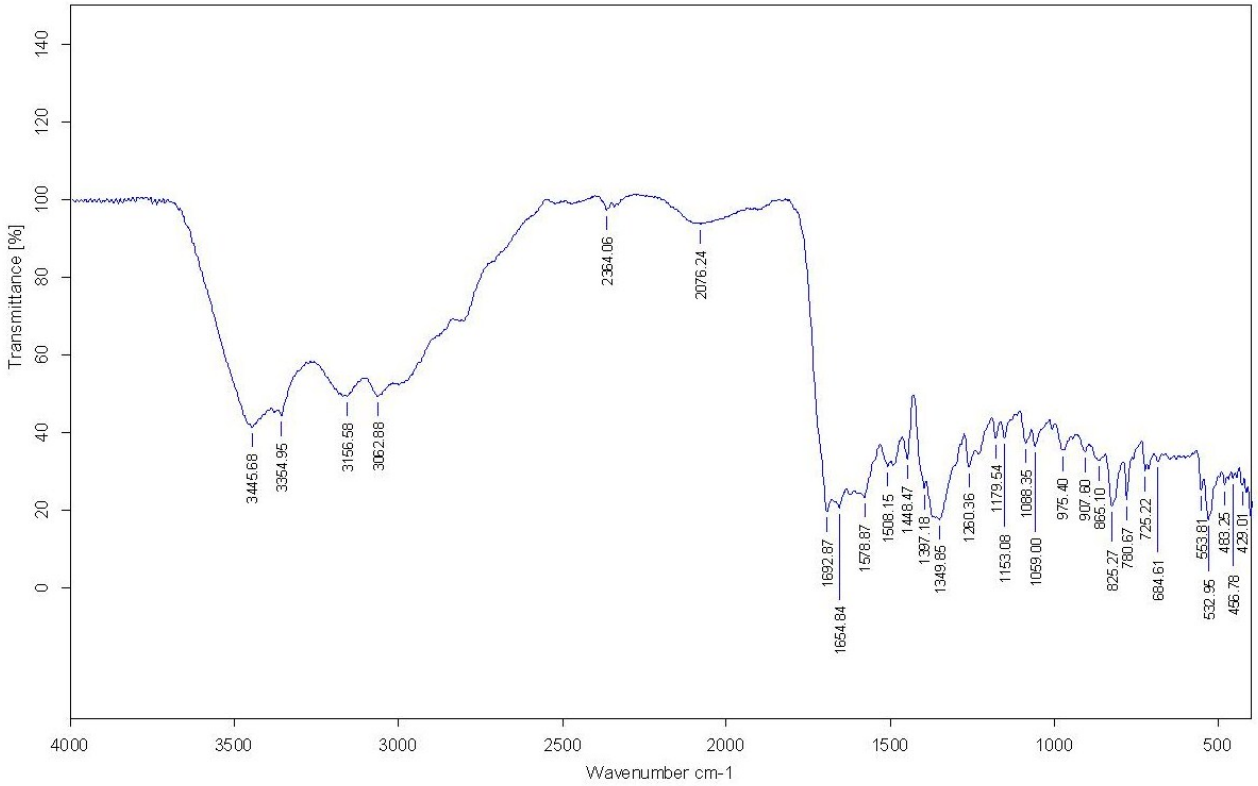

Figure 4S. IR spectra of **2**.

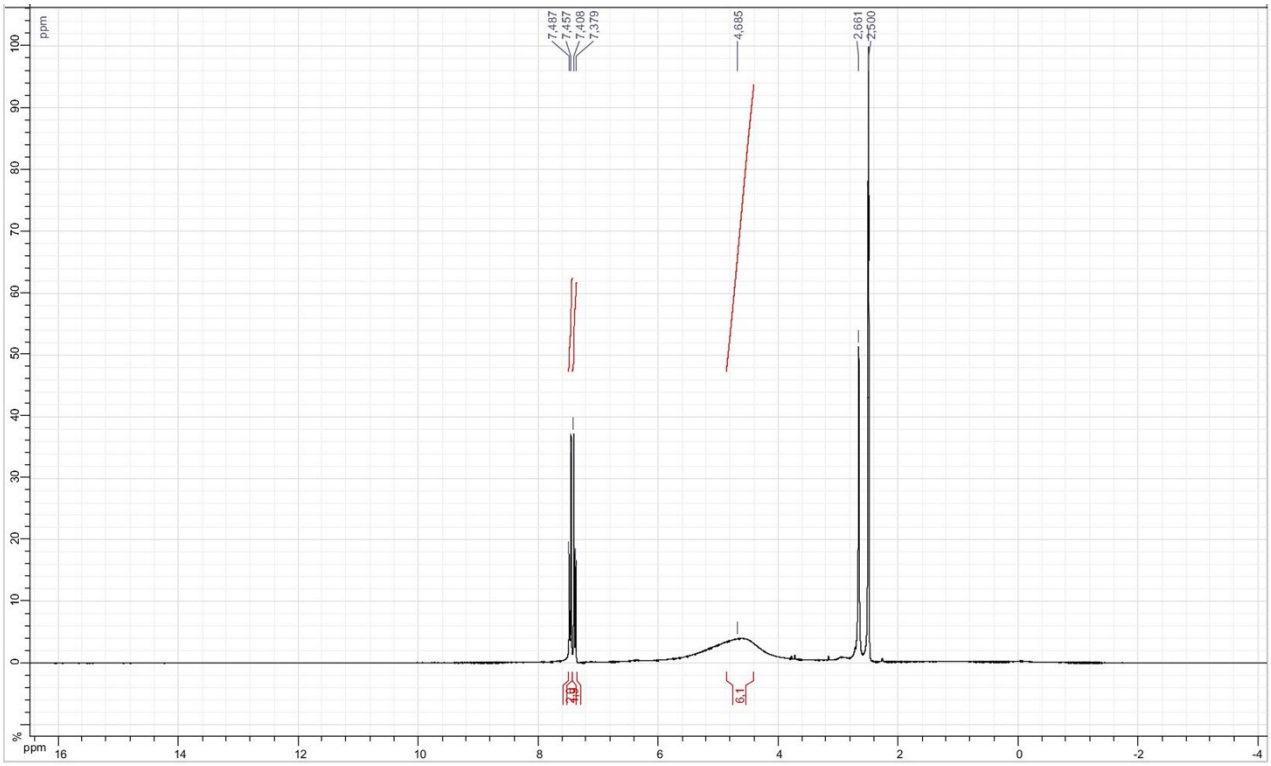

Figure 5S. ^{1}H NMR spectra of **2**.

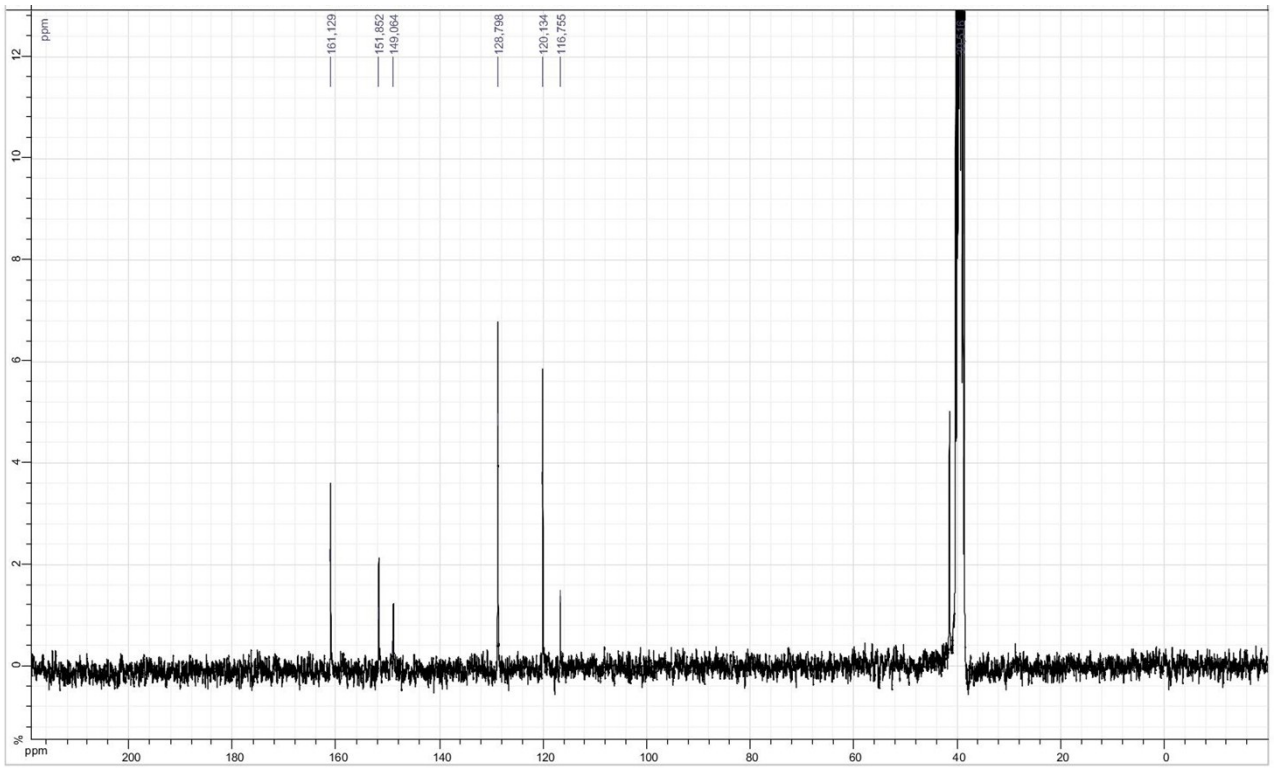

Figure 6S. ^{13}C NMR spectra of **2**.

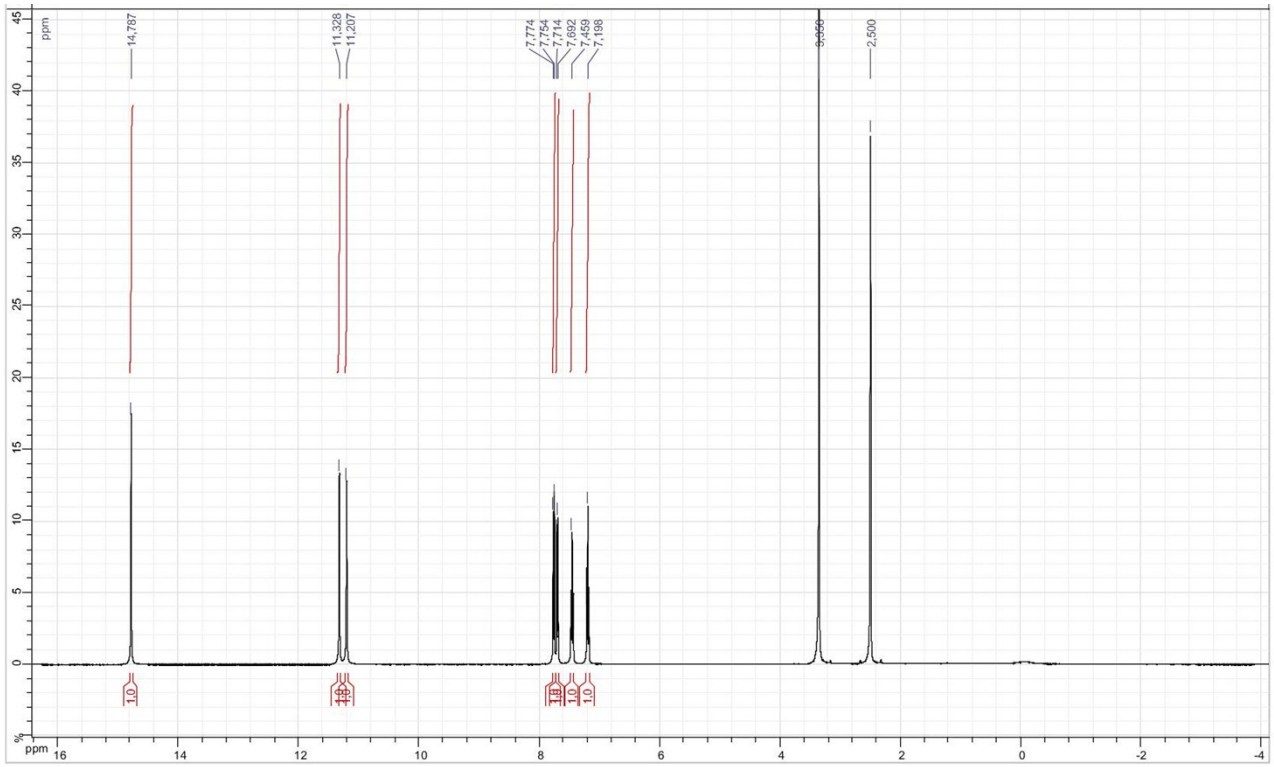

Figure 7S. ^{1}H NMR spectra of **7**.

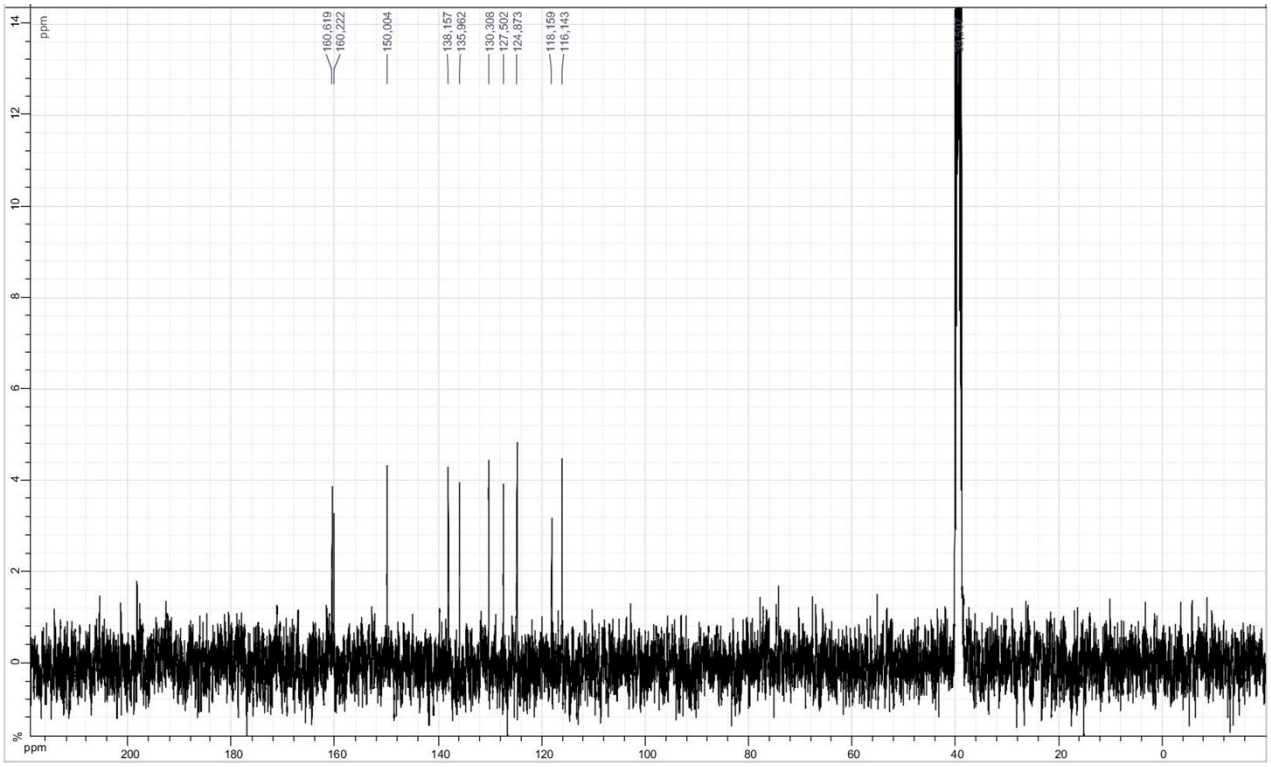

Figure 8S. ^{13}C NMR spectra of **7**.

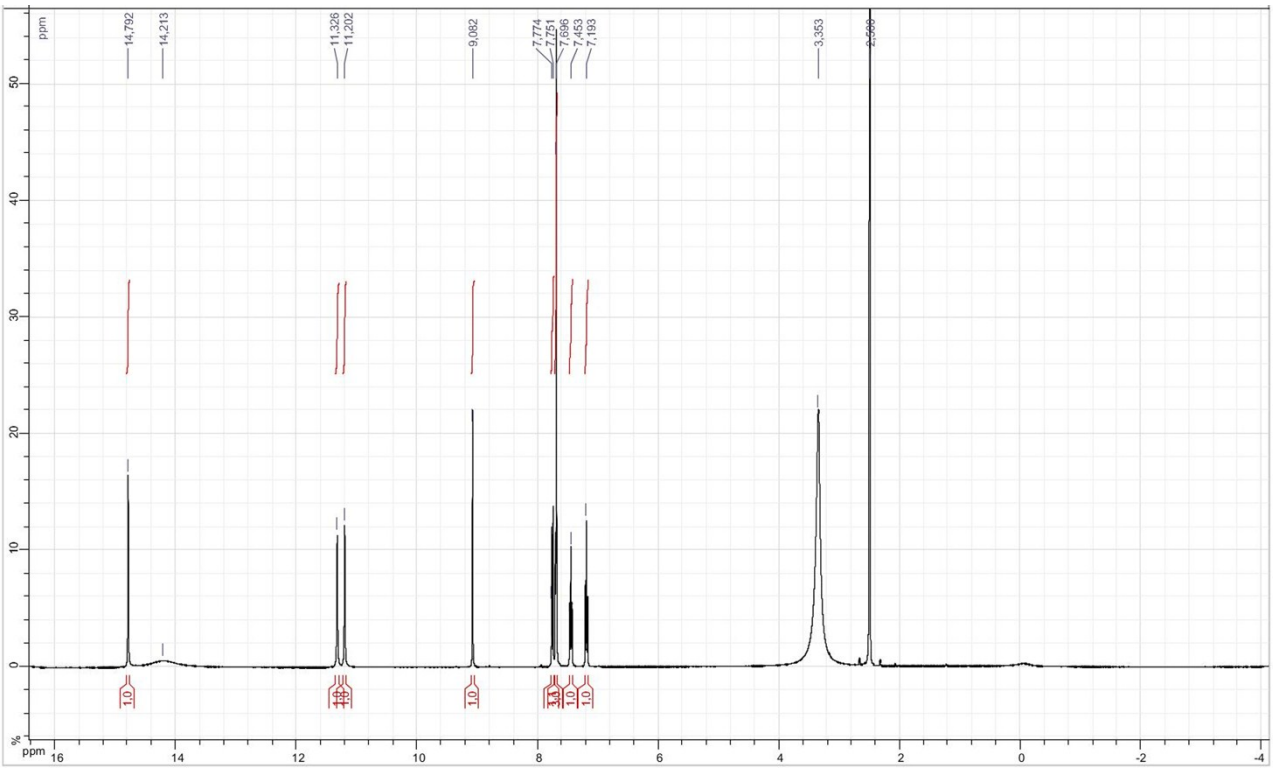

Figure 9S. ^{1}H NMR spectra of **8**.

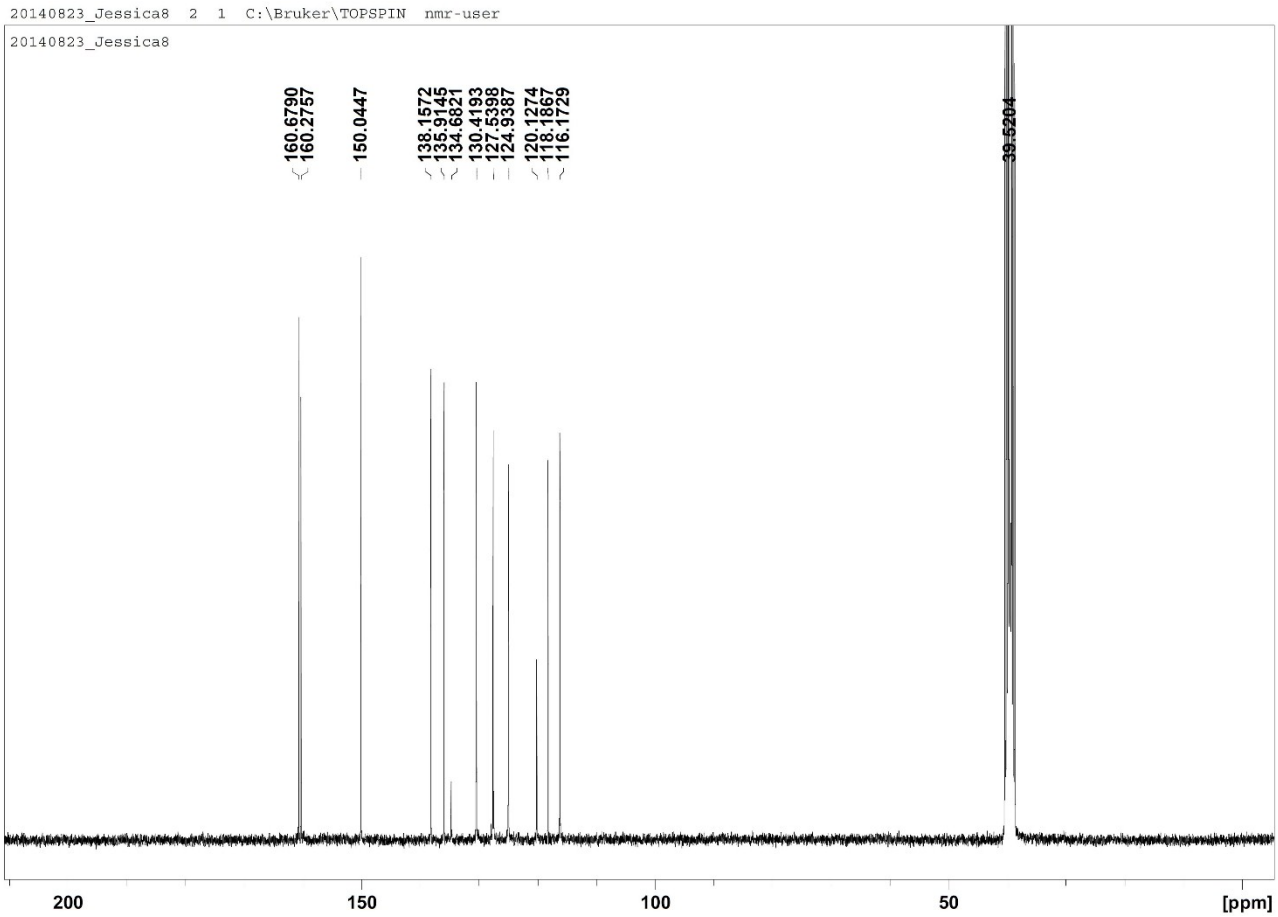

Figure 10S. ^{13}C NMR spectra of **8**.

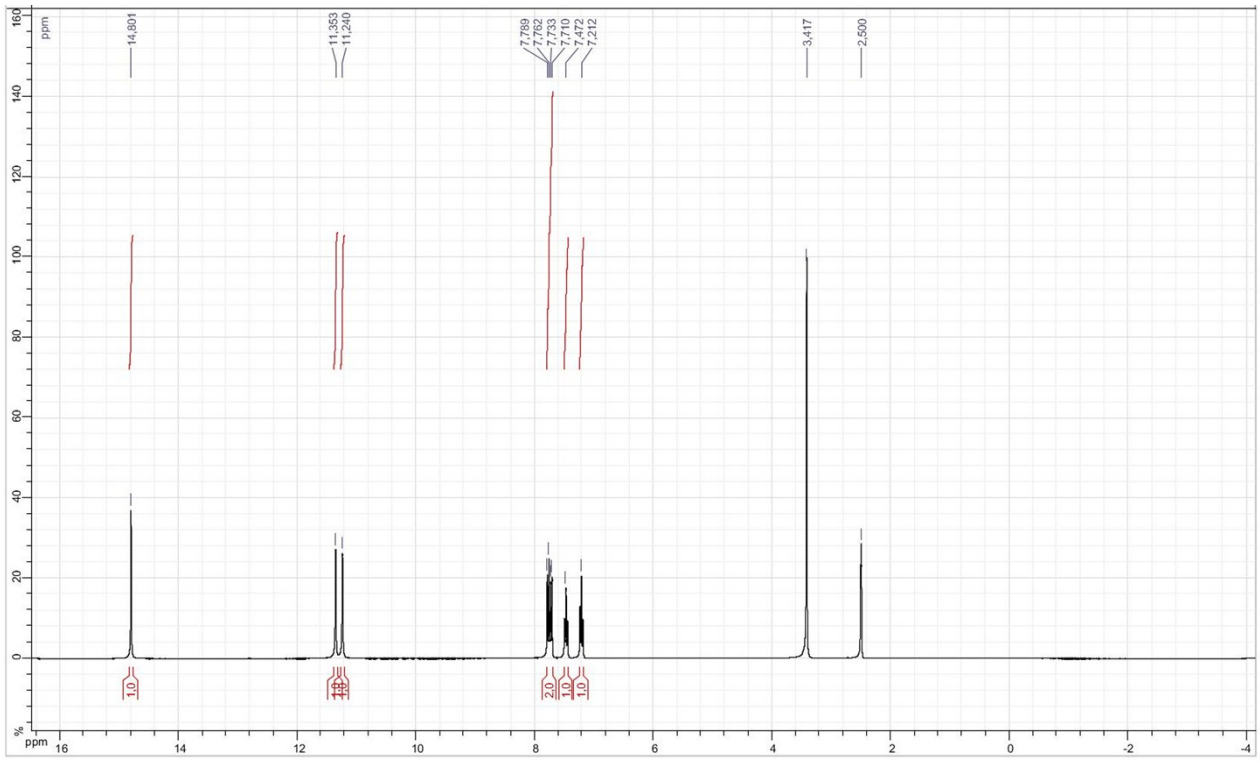

Figure 11S. ^{1}H NMR spectra of **1**.

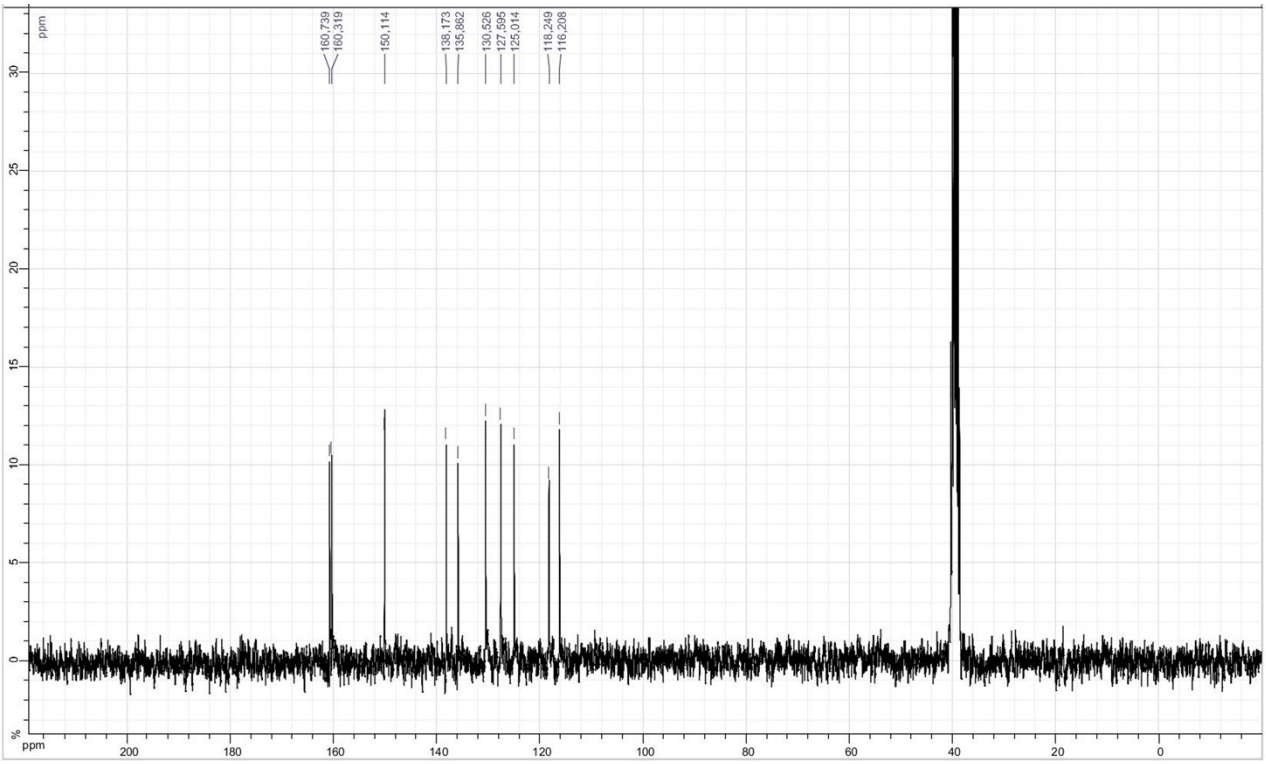

Figure 12S. ^{13}C NMR spectra of **1**.

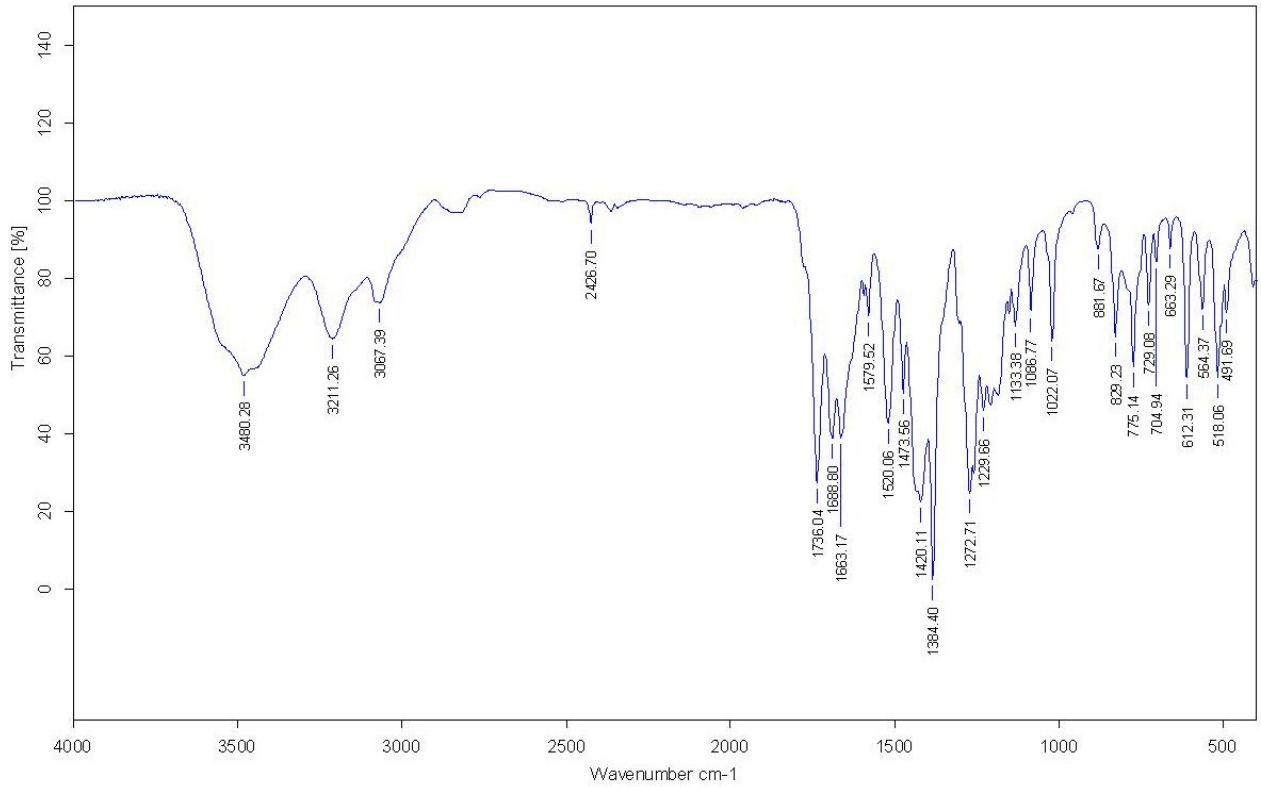

Figure 13S. IR spectra of **7**.

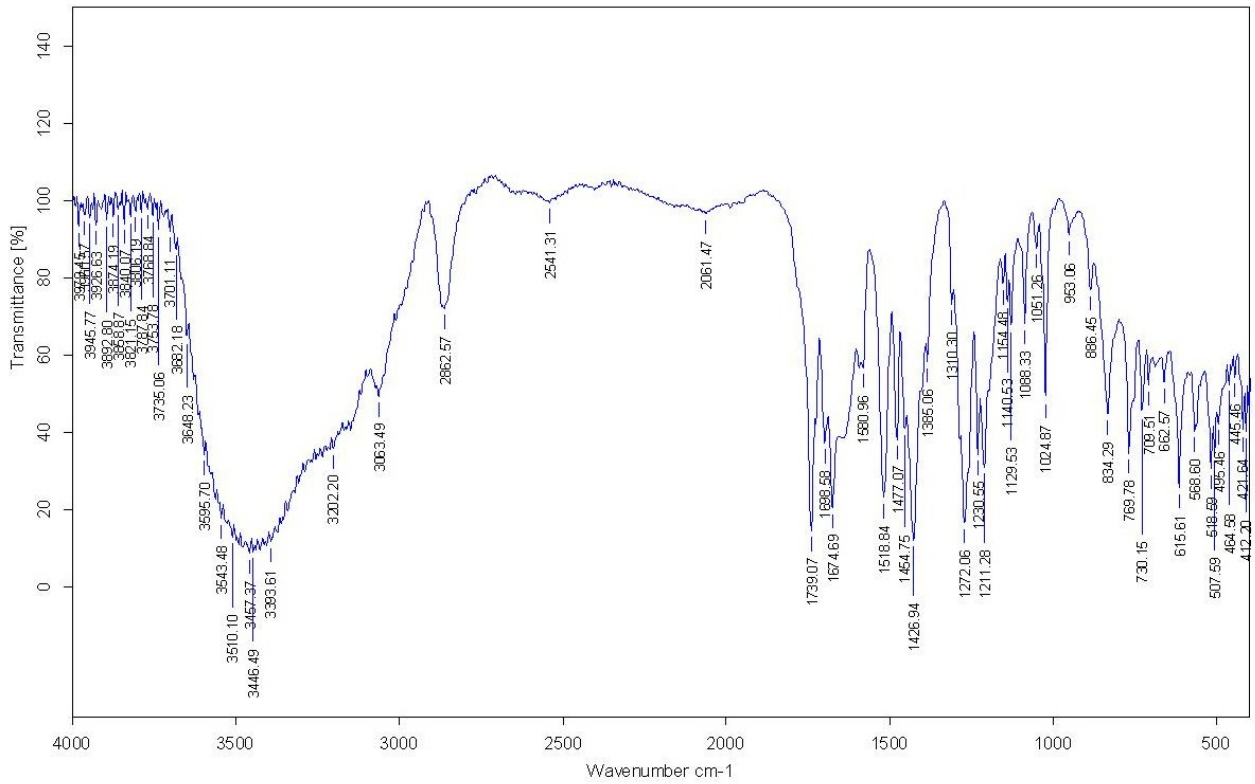

Figure 14S. IR spectra of **8**.

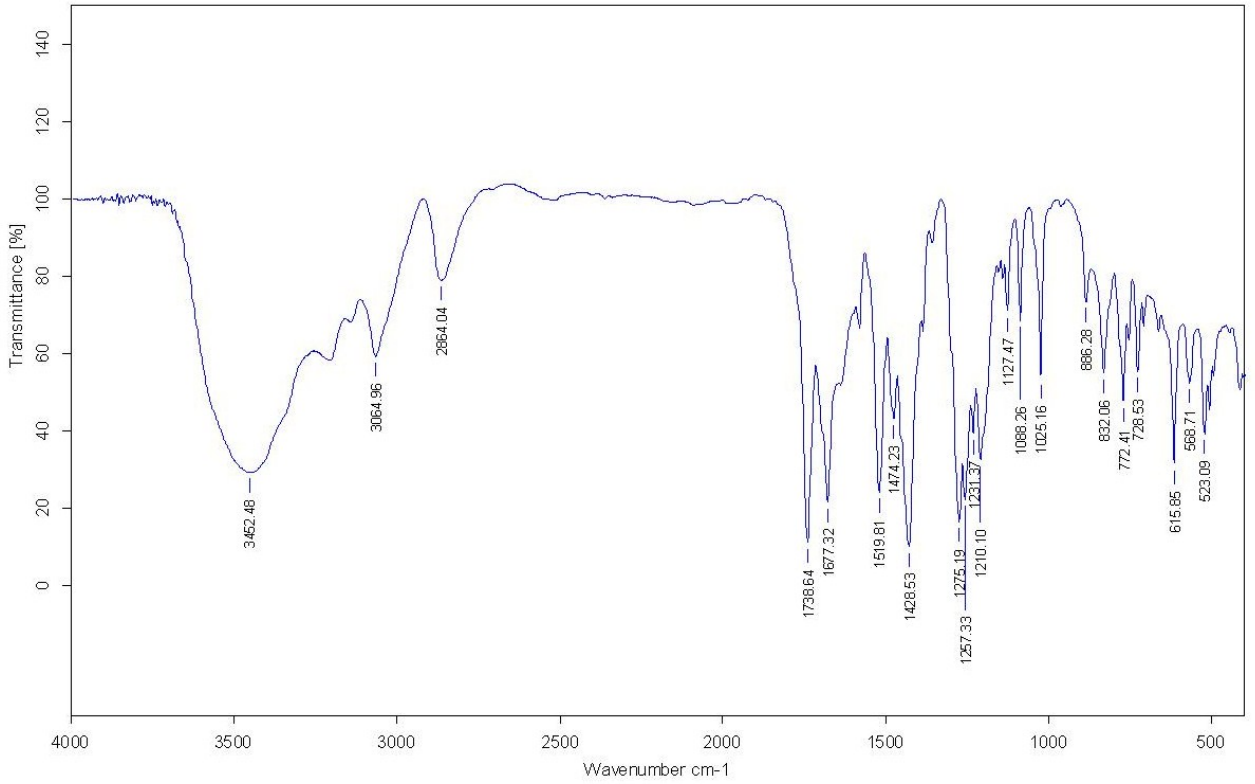

Figure 15S. IR spectra of **1**.

3. X-ray analysis

Table 1S. Crystal data, experimental parameters and selected details of the refinement calculations of compounds **2**, **7** and **8**.

Compound	**2**	**7**	**8**
Empirical formula	$C_{36}H_{49}Cl_3N_{18}O_{11}$	$C_{10}H_9AgN_4O_7S$	$C_{13}H_{16}N_6O_8S$
Formula weight	1016.28	437.14	416.38
Crystal system	Monoclinic	Triclinic	Triclinic
Space group	*P* 21/c	*P* -1	*P* -1
a (Å)	10.4057(3)	8.4530(2)	7.1448(18)
b (Å)	21.2989(6)	9.1802(3)	11.280(4)
c (Å)	21.0249(6)	9.5557(3)	12.049(4)
α (deg)	90	69.666(3)	116.777(12)
β (deg)	100.811(1)	69.858(2)	98.803(11)
γ (deg)	90	79.279(2)	97.186(11)
Z	4	2	2
V (Å^3)	4577.0(2)	650.93(4)	835.8(4)
T (K)	296	150	150
ρcalc (g/cm^3)	1.475	2.230	1.655
μ(Mo Kα) (mm^{-1})	0.279	1.757	0.256
Rfl collected/unique/obs	66617/5164/3794	11649/4749/4228	13696/3413/2364
$R1^a$ ($I \geq 2\sigma$)	0.0857	0.0465	0.0590
$wR2^b$ ($I \geq 2\sigma$)	0.2558	0.1401	0.1523
GOF on F^2	1.135	1.093	0.957

[a] $R1 = \sum||Fo| - |Fc||/\sum|Fo|$. [b] $wR2 = [\sum[w(Fo^2 - Fc^2)2]/\sum[w(Fo^2)^2]]^{1/2}$.

Table 2S. Selected distances (Å) and angles (°) for compounds **2**, **7** and **8**.

2		**7**		**8**	
C8–O1	1.232(7)	C7–N2	1.327(4)	C7–O1	1.232(4)
C9–O2	1.238(7)	C8–O1	1.239(3)	C9–O2	1.217(4)
C7–N2	1.395(8)	C9–O2	1.224(3)	C8–N2	1.326(4)
N1–N2	1.202(8)	O1–Ag1	2.589(3)	C10–O3	1.231(4)
C4–N1	1.498(9)	O3–Ag1	2.566(2)	N1–N2	1.308(4)
C10–O3	1.229(7)	O10–Ag1	2.318(3)	N1–N2–C8	120.5(3)
N2–N1–C4	111.5(7)	O11–Ag1	2.343(2)	N2–C8–C7	124.2(3)
N1–N2–C7	118.1(7)	O13–Ag1	2.359(2)	O1–C7–C8	123.8(3)

Table 3S. Hydrogen bond interactions (Å, º) in complexes **2**, **7** and **8**.

D–H···A	*d*(H···A)	*d*(D···A)	∠(D–H···A)	Symmetry operation
2				
O1W···H1A···O9	1.90(4)	2.758(7)	156(6)	*x,1/2-y,1/2+z*
O2W···H2A···O6	1.91(7)	2.801(6)	167(7)	*x,1/2-y,-1/2+z*
O2W···H2B···O1	2.12(8)	2.821(6)	134(8)	*intra*
O2W···H2B···N1	2.21(6)	2.972(10)	143(9)	*intra*
N3···H3N···O5	1.90(11)	2.900(6)	165(8)	*x,1/2-y,-1/2+z*
N4···H4N···O6	2.08(4)	2.954(6)	170(11)	*x,1/2-y,-1/2+z*
N7···H7N···O3	1.98(3)	2.872(6)	177(15)	*1+x,1/2-y,1/2+z*
N8···H8N···O1	1.84(11)	2.814(6)	174(10)	*x,1/2-y,1/2+z*
N11···H11N···O7	1.96(12)	2.824(6)	166(8)	*1-x,1-y,1-z*
N12···H12N···O9	2.08(12)	2.938(6)	164(9)	*-x,1-y,1-z*
N31···H31C···O2	2.08(7)	2.868(7)	148(9)	*intra*
N31···H31D···O1W	2.19(11)	3.042(9)	148(10)	*intra*
N32···H32C···O2	2.52(11)	3.118(7)	122(8)	*intra*
N32···H32C···N2	2.38(11)	3.296(8)	164(9)	*intra*
N32···H32D···O5	2.28(10)	3.011(7)	133(8)	*intra*
N32···H32D···N6	2.31(11)	3.193(7)	154(9)	*intra*
N32···H32E···N35	1.88(11)	2.836(8)	172(5)	*-1+x,y,z*
N33···H33C···O5	2.34	3.175(8)	156	*intra*
N33···H33D···O8	2.37	3.094(7)	138	*intra*
N34···H34C···N31	1.84(11)	2.811(9)	168(10)	*-x,1/2+y,3/2-z*
N34···H34D···O2W	1.90(8)	2.785(8)	170(8)	*1-x,1/2+y,3/2-z*
N34···H34E···O8	2.38(11)	2.940(7)	125(9)	*intra*
N34···H34E···N9	2.28(11)	3.074(8)	159(9)	*intra*
N35···H35C···O4	2.42(12)	2.992(7)	124(10)	*intra*
N36···H36C···O1W	2.40(11)	2.991(9)	122(7)	*1-x,1/2+y,3/2-z*
N36···H36D···O7	1.93(8)	2.810(7)	170(8)	*intra*
N36···H36E···O4	2.13(10)	2.770(7)	124(8)	*intra*
N36···H36E···N5	2.13(12)	2.976(8)	149(10)	*intra*
7				
N1···H1N···O1	1.87(4)	2.613(4)	142(6)	*intra*
N1···H1N···O13	2.22(6)	2.815(4)	125(5	*intra*
N3···H3N···O12	2.17(3)	3.037(4)	166(6)	*1-x,1-y,1-z*
N4···H4N···O13	2.50(6)	3.059(4)	121(5)	*x,1+y,z*
N4···H4N···O2	2.09(6	2.912(4)	153(5)	*1-x,2-y,2-z*
O10···H10A···O11	1.98(5)	2.911(5)	159(5)	*-x,1-y,1-z*
O10···H10B···.O2	1.86(5)	2.815(4)	169(4)	*x,y,-1+z*
8				
O1W···H1W1···O12	2.02(4)	2.830(4)	159(4)	*intra*
N1···H1N···O1	2.01(5)	2.650(5)	124(4)	*intra*
N1···H1N···O13	1.94(4)	2.714(4)	138(4)	*intra*
O1W···H1W2···O11	2.27(4)	2.934(4)	146(5)	*1+x,y,z*
O2W···H2W1···O3	1.88(3)	2.842(3)	166(4)	*1-x,1-y,-z*
N3···H3N···O1W	1.87(4)	2.776(4)	178(5)	*-1+x,y,-1+z*
O2W···H2W2···O11	1.83(2)	2.718(4)	175(3)	*1-x,1-y,1-z*
N4···H4N···O3	2.09(4)	2.911(4)	175(5)	*1-x,1-y,-z*
N11···H11N···O2W	1.84(4)	2.706(4)	172(4)	*intra*
N12···H12N···O13	2.21(4)	2.798(4)	127(4)	*-1+x,y,z*
N12···H12N···O2	2.19(5)	2.888(5)	140(3)	*-x,-y,-z*

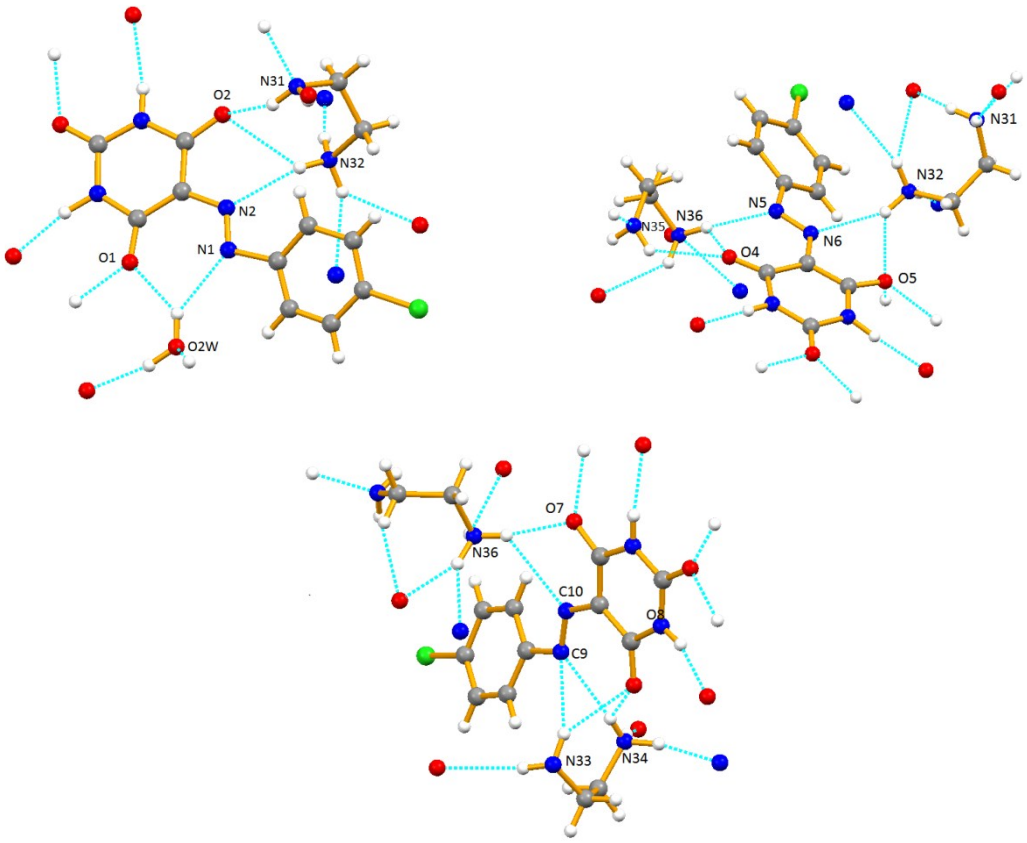

Figure 16S. Hydrogen bond interactions in **2** (in dashed blue lines; see also Table 3S) grouped by hydrazonium anion and monoprotonated ethylenediamine cation.

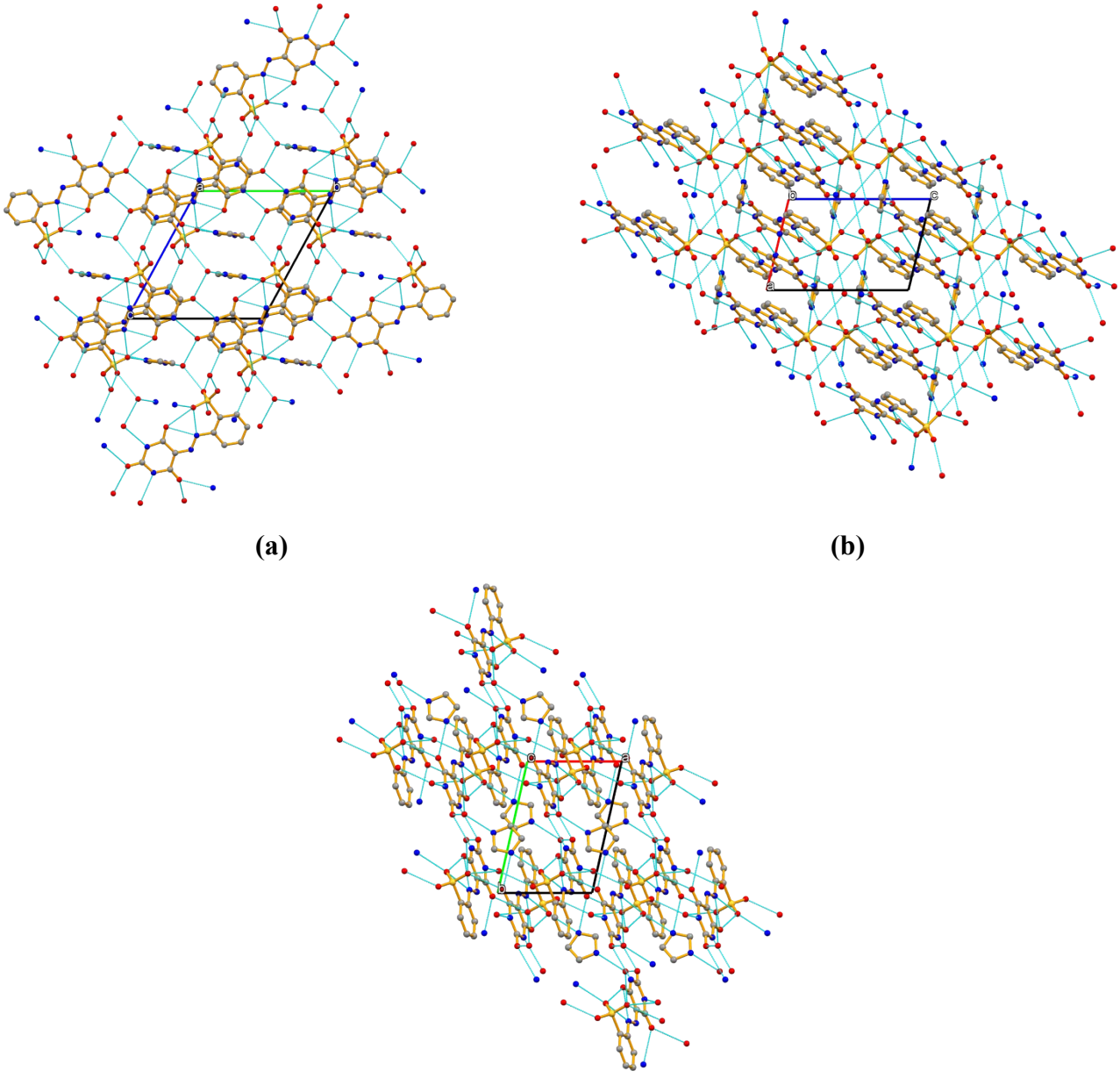

Figure 17S. 3D network arrangement in **2** viewed down the crystallographic *a*, *b* and *c* axis, respectively. Hydrogen atoms were omitted for clarity.

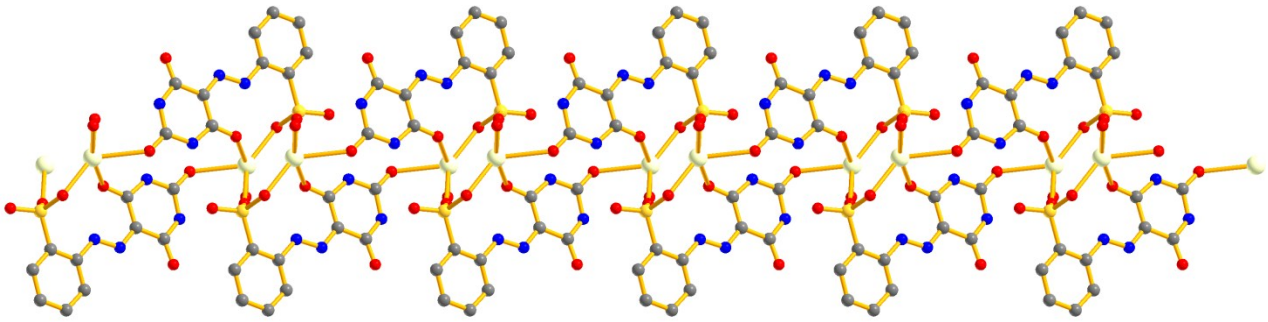

Figure 18S. 1D polymeric chain arrangement in **7**. Hydrogen atoms were omitted for clarity.

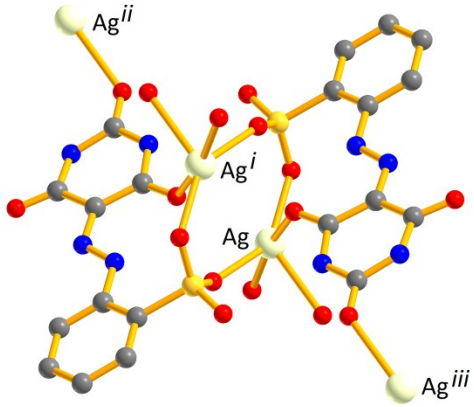

Figure 19S. The bridging mode of the sulfonyl groups in **7** which generate $\{Ag_2S_2O_4\}$ dimetallic cores. i) 1-x,1-y,1-z; ii) x,-1+y,z; iii) 1-x,2-y,1-z

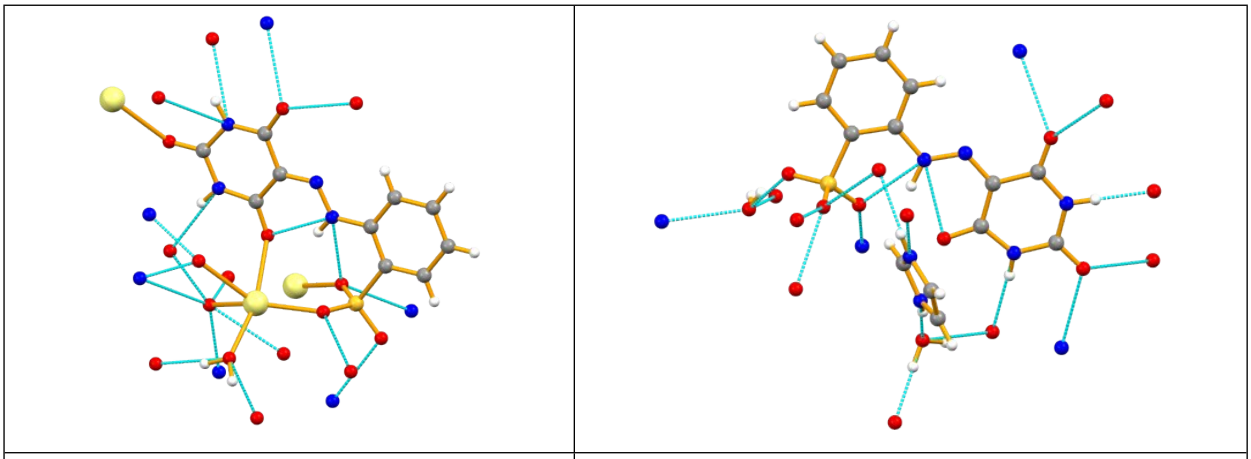

7	**8**

Figure 20S. Hydrogen bond interactions (in dashed blue lines; see also Table 3S) in **7** and **8**.

4. Electronic absorption spectra

Table 4S. Electronic absorption spectral data of proligands H_4L^1 and H_3L^2 and complexes **1**−**9**.

Compound	λ_{max} (nm)	ε (M^{-1} cm^{-1})×10^{-3}
H_4L^1	414	37.6
	266	8.10
H_3L^2	388	37.5
	262	7.51
1	389	50.1
	234	2.41
2	388	76.5
	262	16.9
3	480	23.0
	366	12.5
	269	15.7
4	424	72.2
	350	25.3
	269	63.4
5	393	18.3
	350	14.9
	260	16.3
6	388	21.6
	265	6.04
7	388	21.1
8	388	33.3
	262	13.2
9	384	64.1
	262	20.2

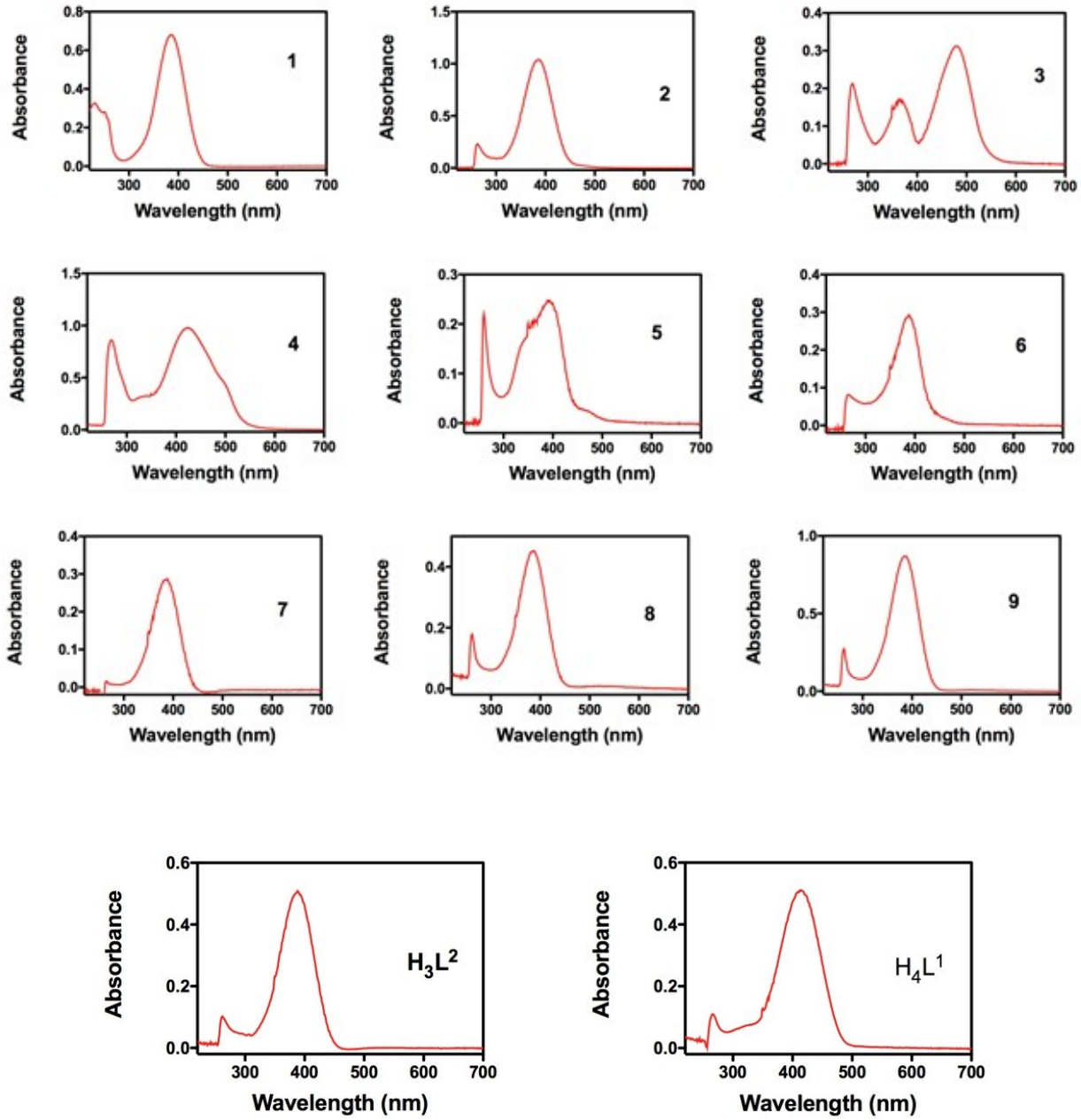

Figure 21S. UV–vis spectra for different compounds 15 μM in DMSO (**H_4L^1, H_3L^2, 2-9**) and water (**1**) solution.

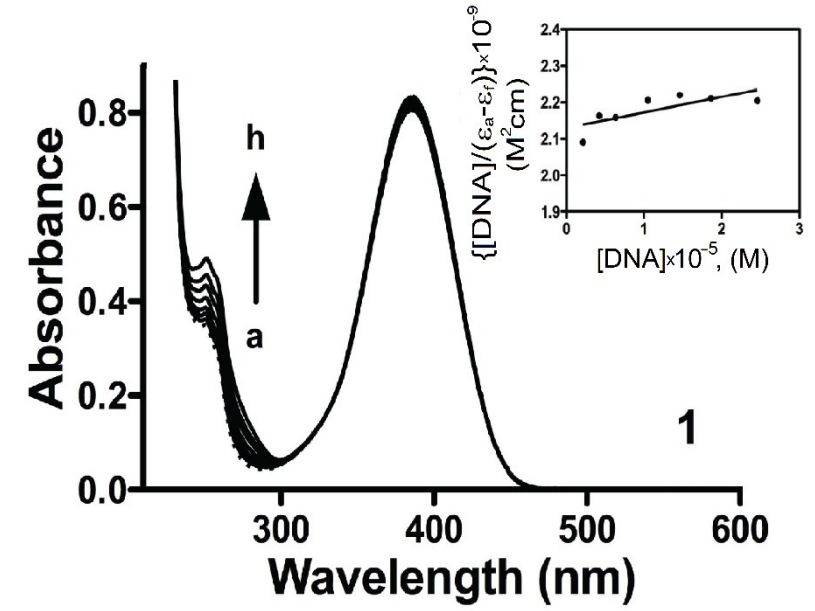
Absorbance
Wavelength (nm)
h
a
1
{[DNA]/(εa-εf)}×10-9 (M2cm)
[DNA]×10-5, (M)

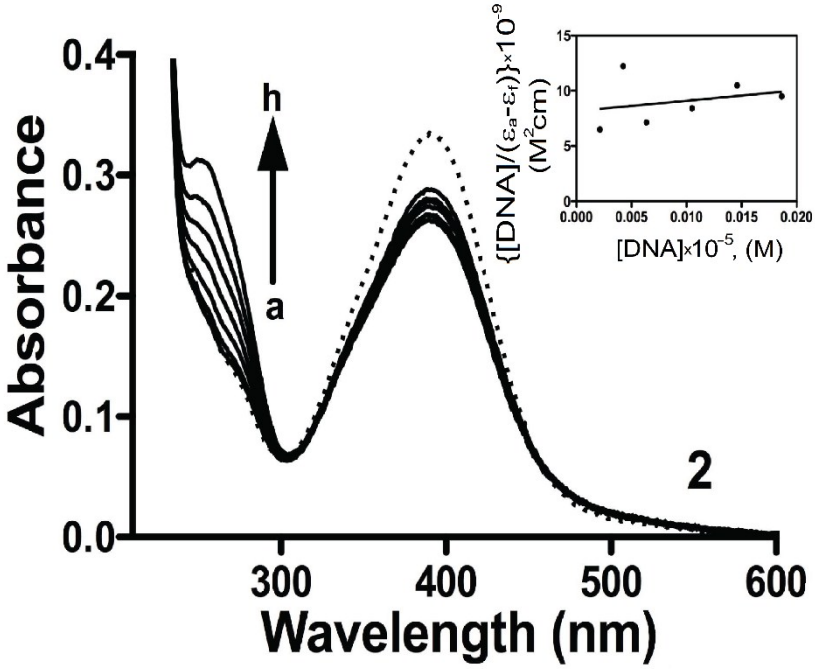
Absorbance
Wavelength (nm)
h
a
2
{[DNA]/(εa-εf)}×10-9 (M2cm)
[DNA]×10-5, (M)

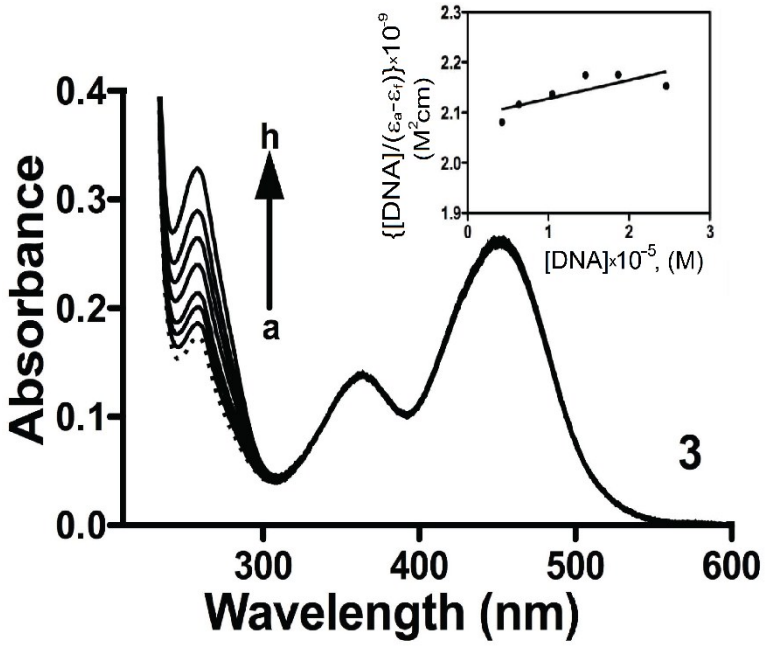
Absorbance
Wavelength (nm)
h
a
3
{[DNA]/(εa-εf)}×10-9 (M2cm)
[DNA]×10-5, (M)

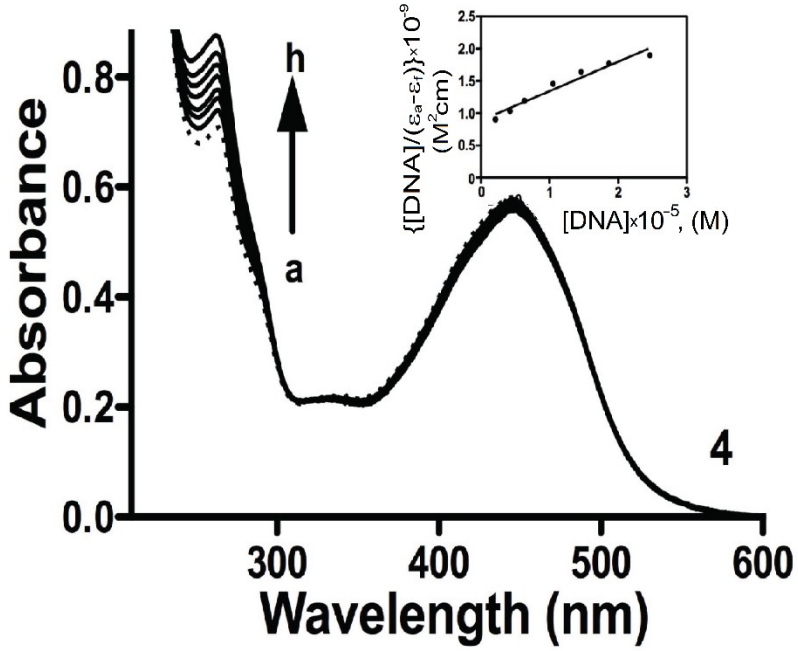
Absorbance
Wavelength (nm)
h
a
4
{[DNA]/(εa-εf)}×10-9 (M2cm)
[DNA]×10-5, (M)

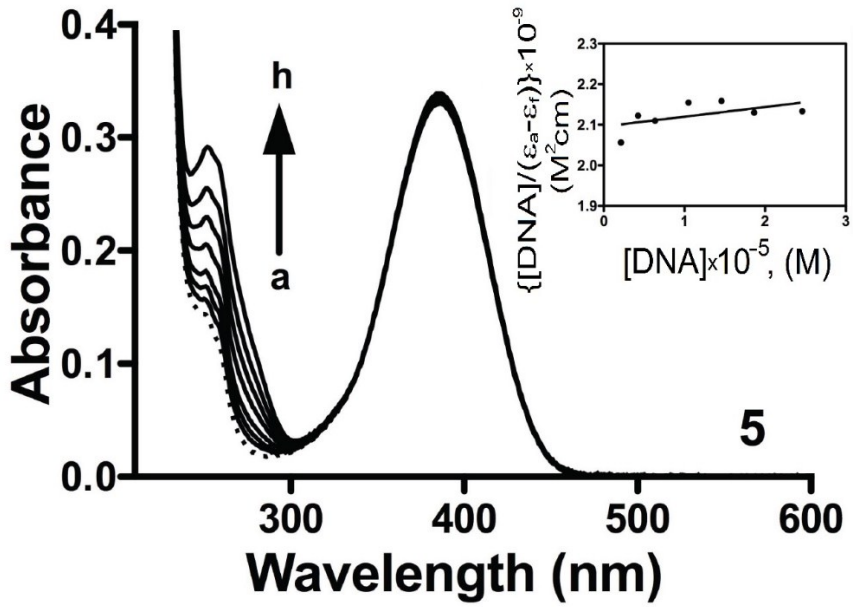
Absorbance
Wavelength (nm)
h
a
5
{[DNA]/(εa-εf)}×10-9 (M2cm)
[DNA]×10-5, (M)

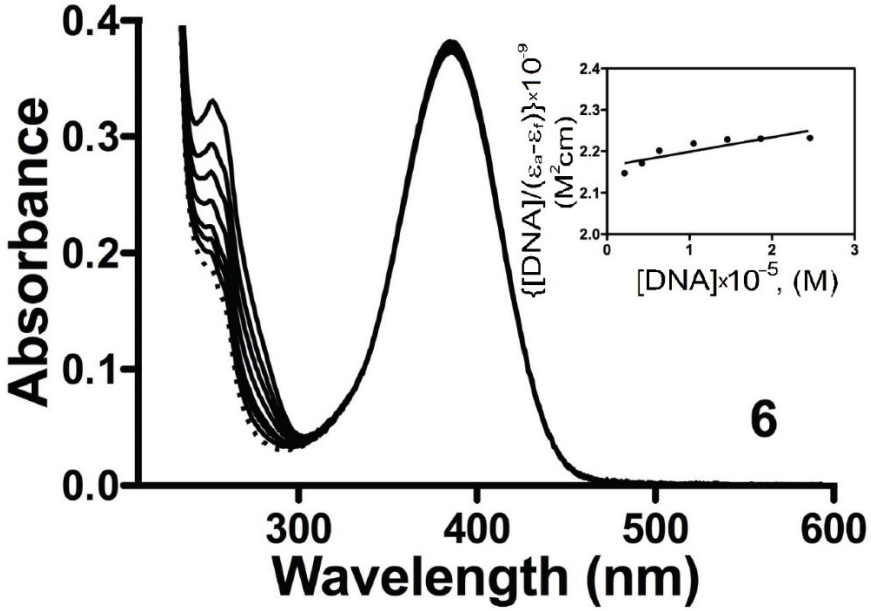
Absorbance
Wavelength (nm)
6
{[DNA]/(εa-εf)}×10-9 (M2cm)
[DNA]×10-5, (M)

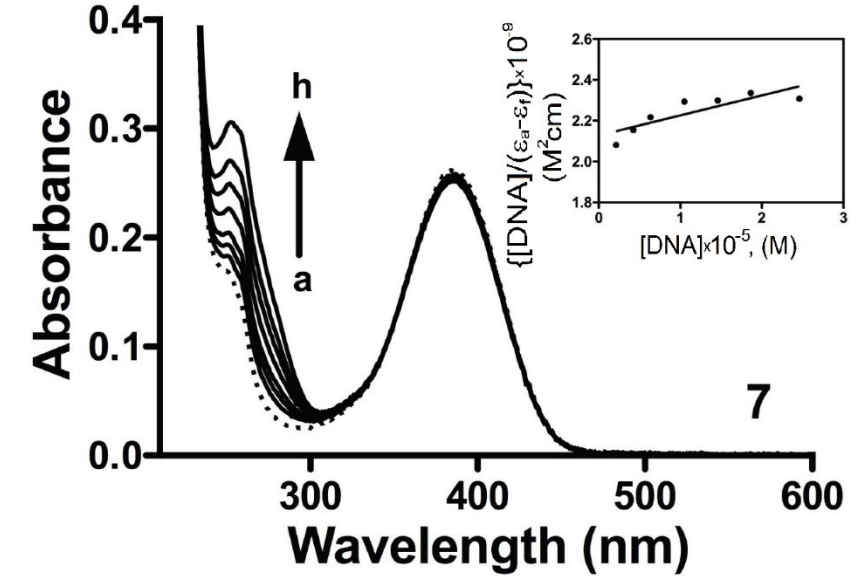
Absorbance
Wavelength (nm)
h
a
7
{[DNA]/(εa-εf)}×10-8 (M2cm)
[DNA]×10-5, (M)

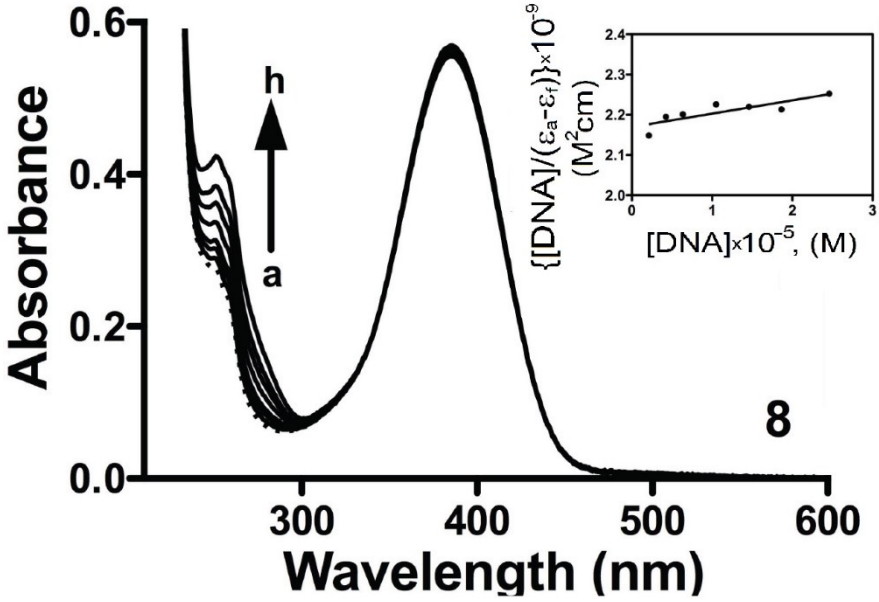
Absorbance
Wavelength (nm)
h
a
8
{[DNA]/(εa-εf)}×10-9 (M2cm)
[DNA]×10-5, (M)

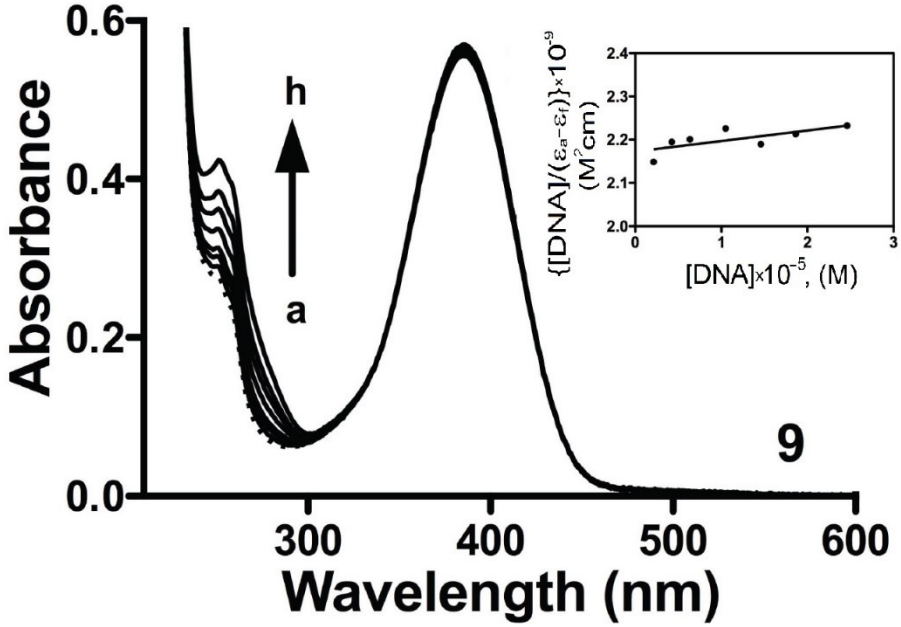
Absorbance
Wavelength (nm)
h
a
9
{[DNA]/(εa-εf)}×10-9 (M2cm)
[DNA]×10-5, (M)

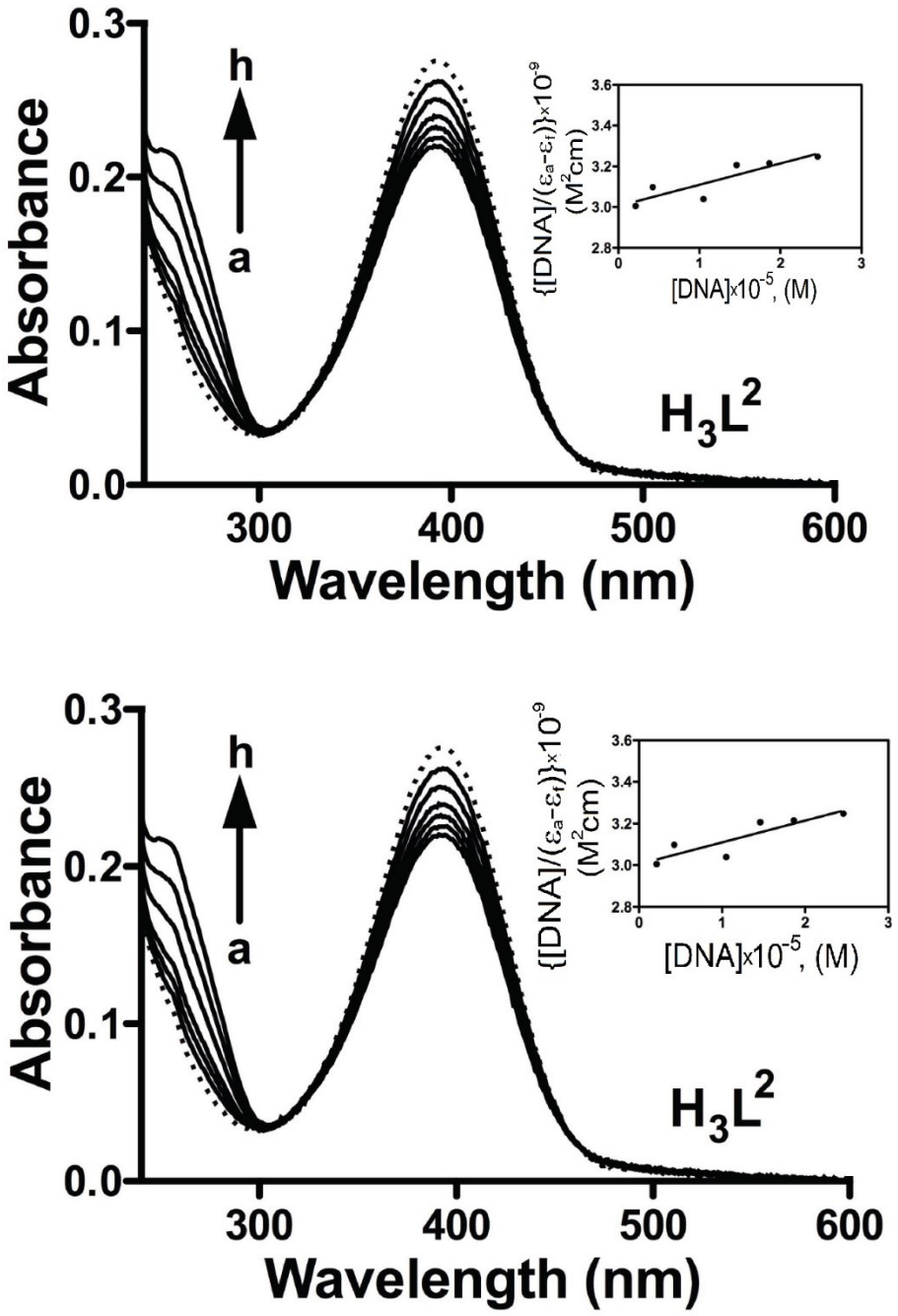

Figure 22S. Absorption spectral traces of different complexes (**panel A**) and ligands **(panel B)** in phosphate buffer (10mM, pH 7.2) after gradual addition of calf thymus DNA (from a = 0 to h = 24 mM). Inset shows the plot of $[DNA]/|\varepsilon_a - \varepsilon_f|$ *vs.* [DNA] (equation 1).

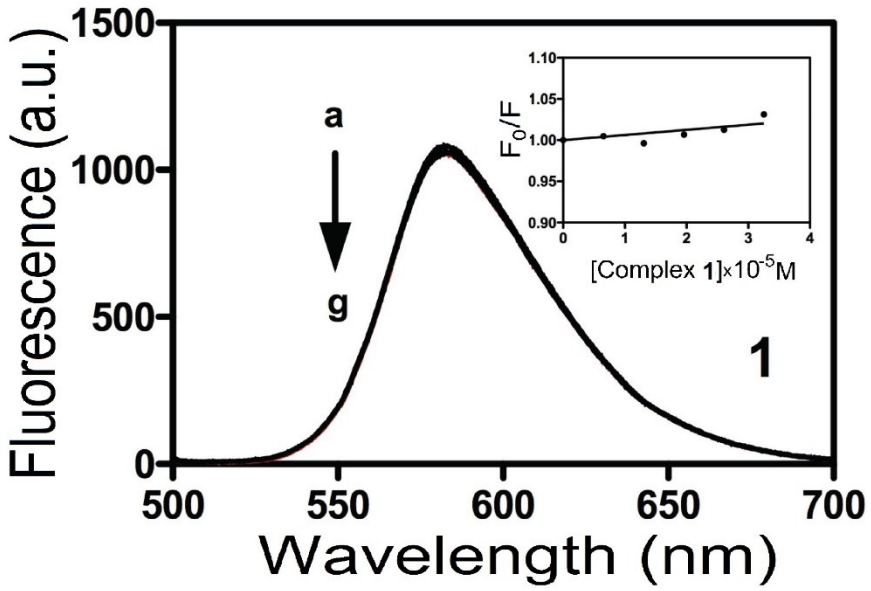
Fluorescence (a.u.)
1500
1000
500
0
500
550
600
650
700
Wavelength (nm)
a
g
1
F_0/F
1.10
1.05
1.00
0.95
0.90
0
1
2
3
4
[Complex 1]×10^{-5}M

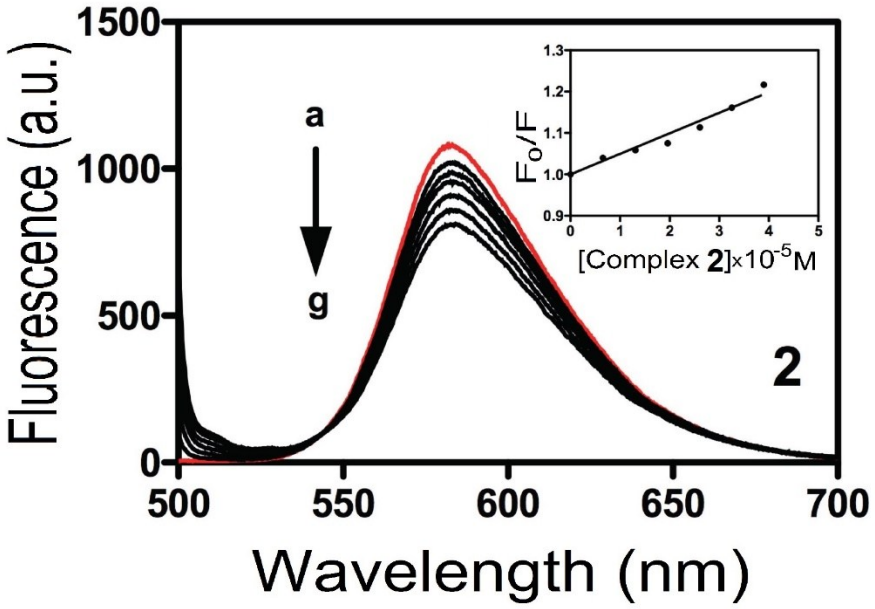
Fluorescence (a.u.)
1500
1000
500
0
500
550
600
650
700
Wavelength (nm)
a
g
2
F_0/F
1.3
1.2
1.1
1.0
0.9
0
1
2
3
4
5
[Complex 2]×10^{-5}M

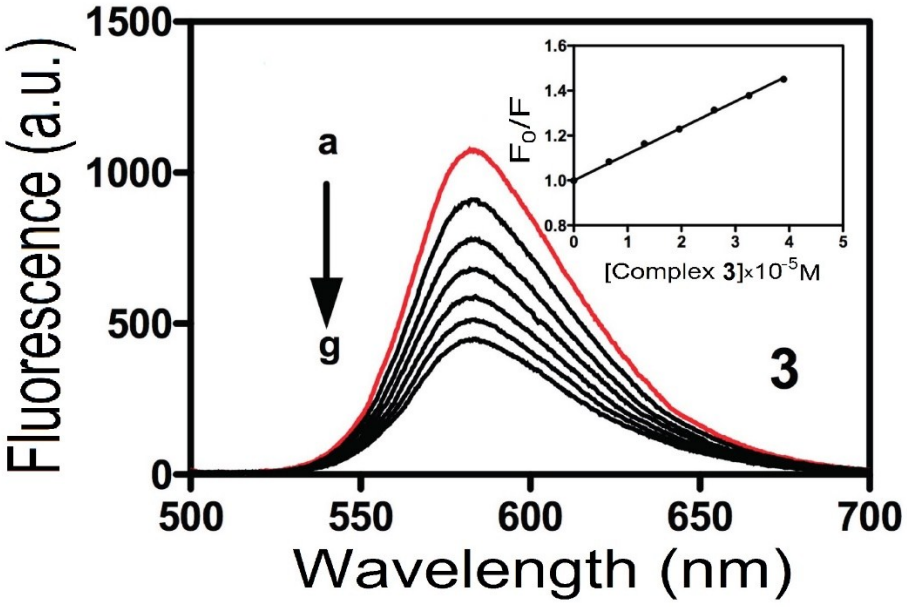
Fluorescence (a.u.)
1500
1000
500
0
500
550
600
650
700
Wavelength (nm)
a
g
3
F_0/F
1.6
1.4
1.2
1.0
0.8
0
1
2
3
4
5
[Complex 3]×10^{-5}M

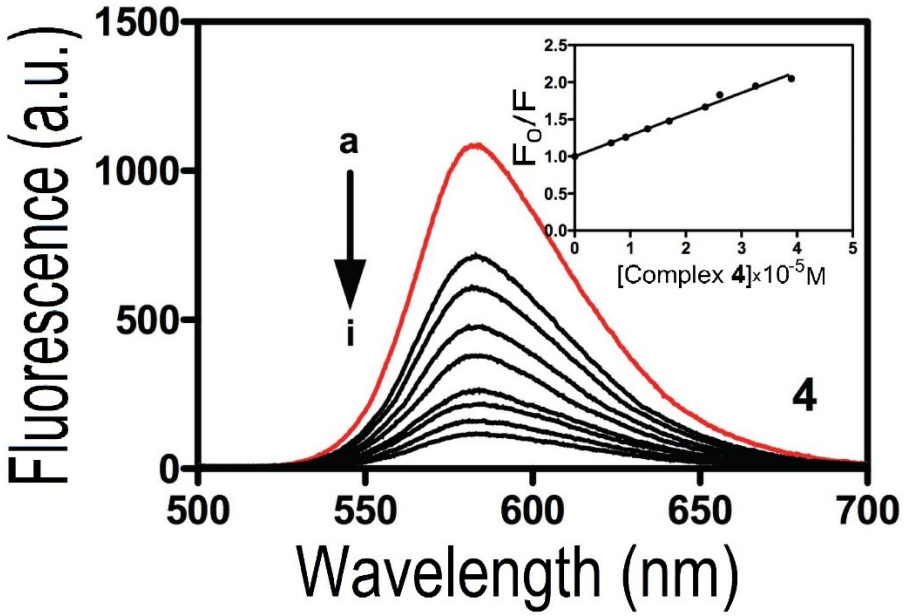
Fluorescence (a.u.)
Wavelength (nm)
a
i
4
F_o/F
[Complex 4]×10^{-5}M

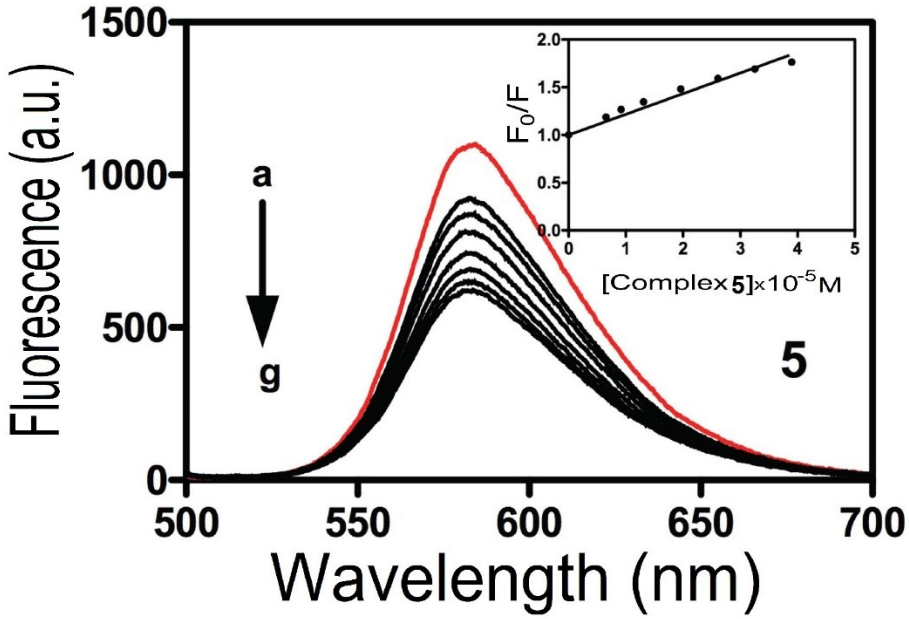
Fluorescence (a.u.)
Wavelength (nm)
a
g
5
F_o/F
[Complex 5]×10^{-5}M

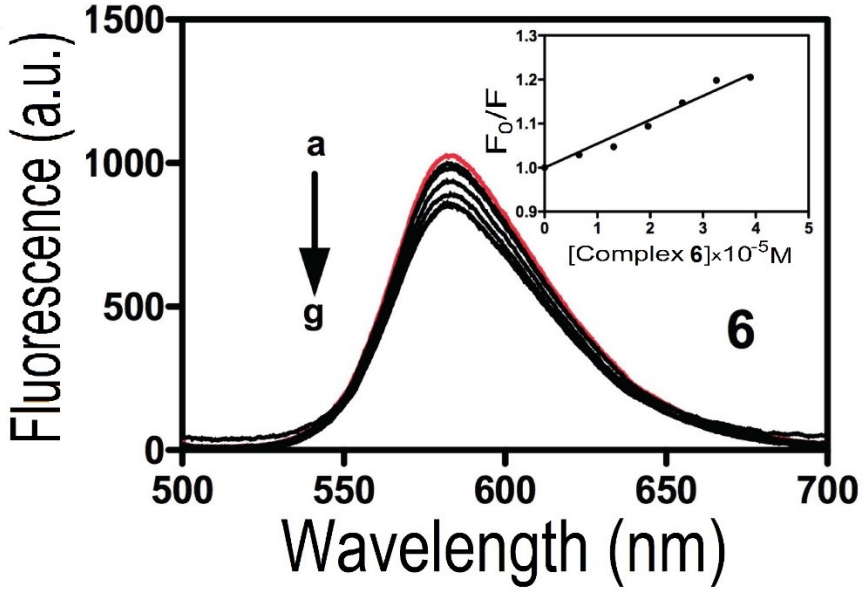
Fluorescence (a.u.)
Wavelength (nm)
a
g
6
F_o/F
[Complex 6]×10^{-5}M

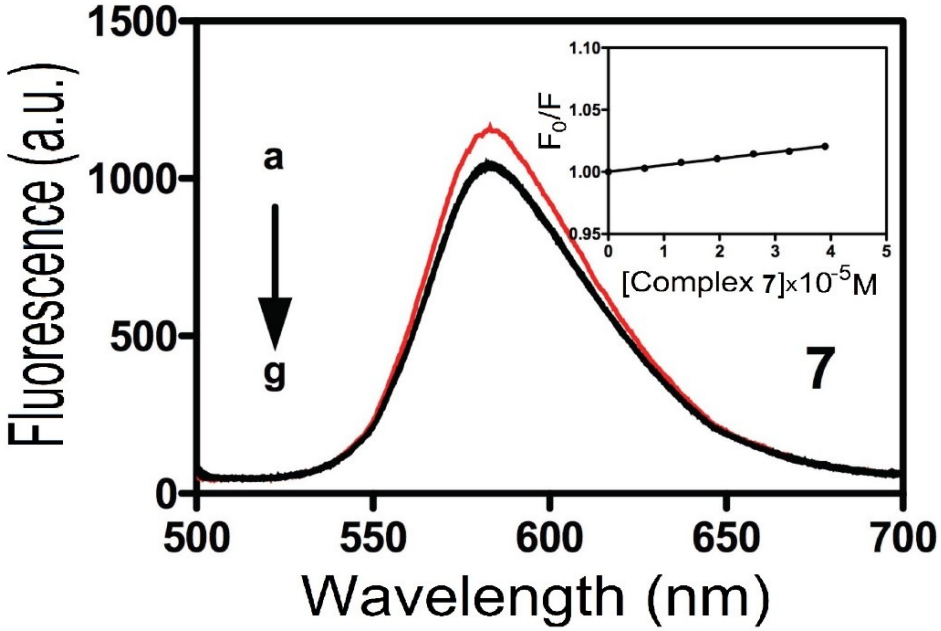
Fluorescence (a.u.)
Wavelength (nm)
a
g
7
F_0/F
[Complex 7]×10^{-5}M

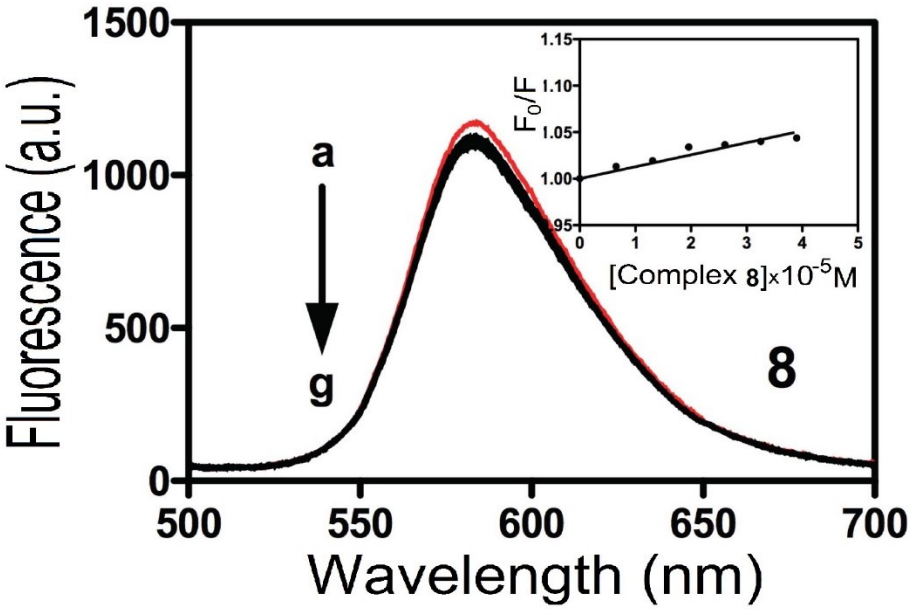
Fluorescence (a.u.)
Wavelength (nm)
a
g
8
F_0/F
[Complex 8]×10^{-5}M

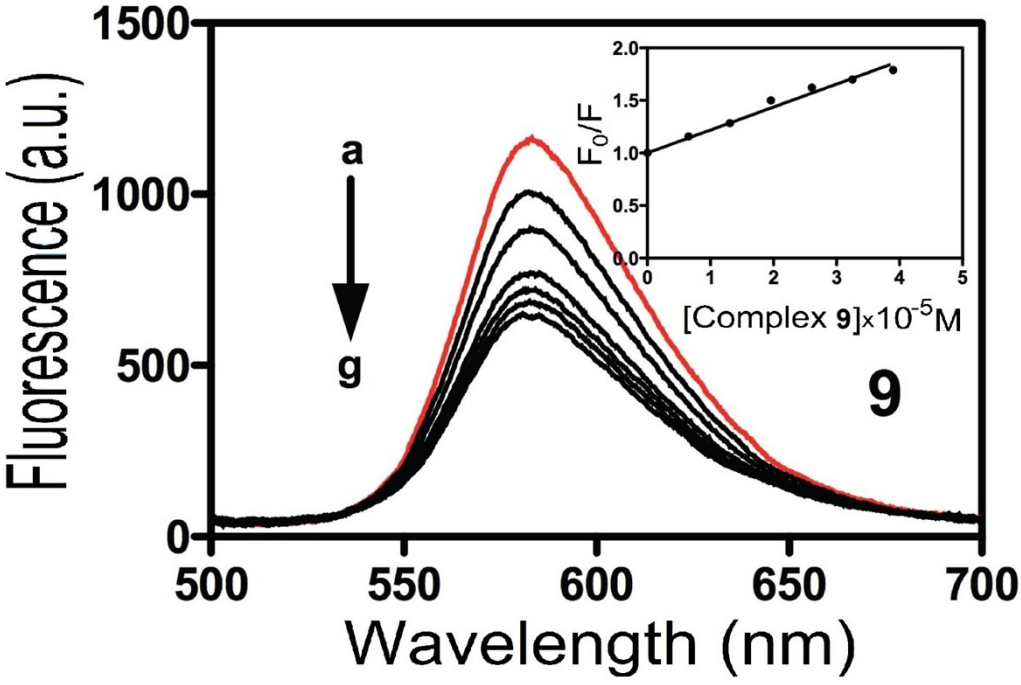
Fluorescence (a.u.)
Wavelength (nm)
a
g
9
F_0/F
[Complex 9]×10^{-5}M

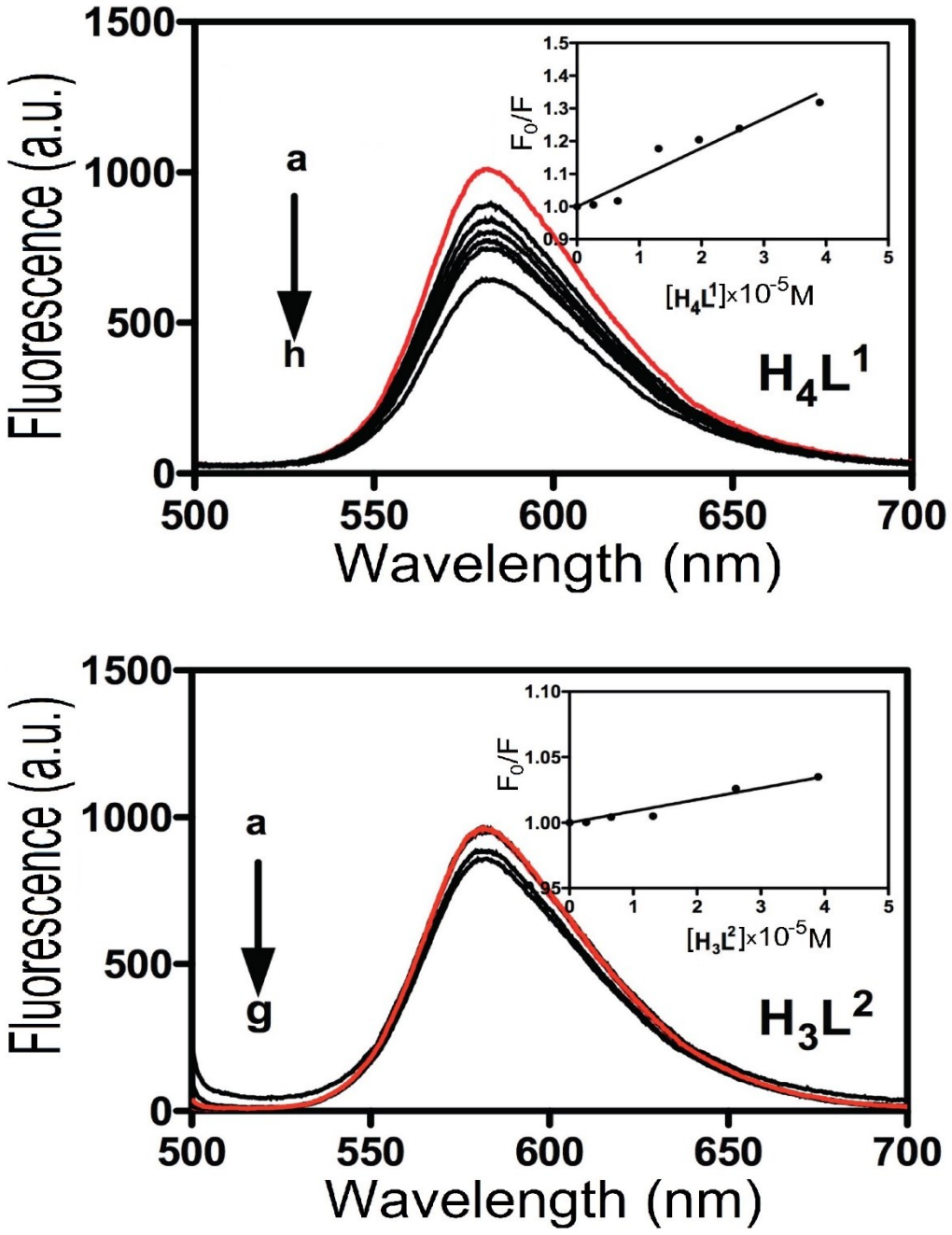

Figure 23S. Emission spectra of EB bound to ct-DNA upon excitation at 490 nm in the presence of increasing concentration of different complexes from (a) 0 to (g) 39 μM; ([EB] = 6 μM, [ct-DNA] = 50 μM. Inset: Stern Volmer plot of $\mathbf{F_0/F}$ vs. [complex] for the titration of the complexes to EB-ct-DNA complex.

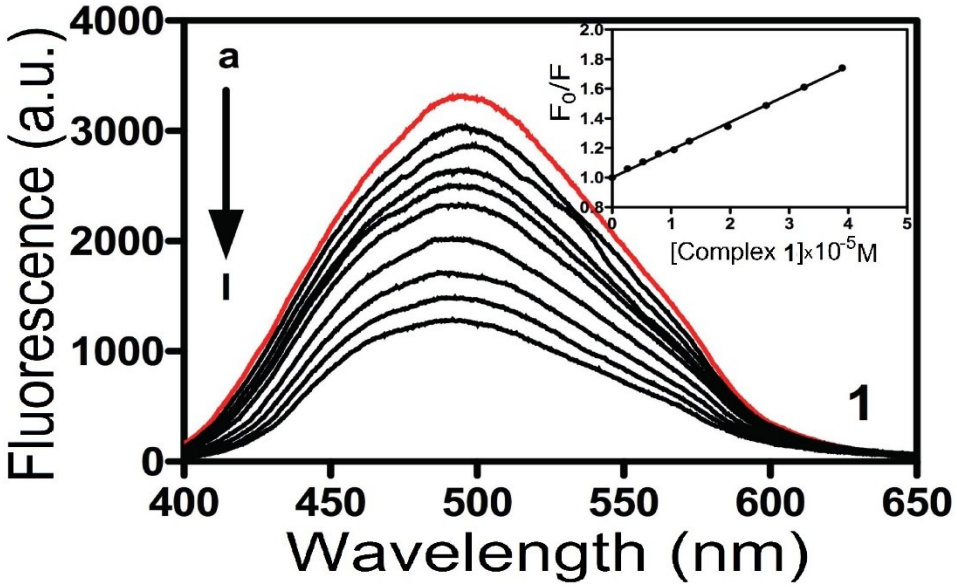
Fluorescence (a.u.)
Wavelength (nm)
a
I
1
F_0/F
[Complex 1]×10^{-5}M

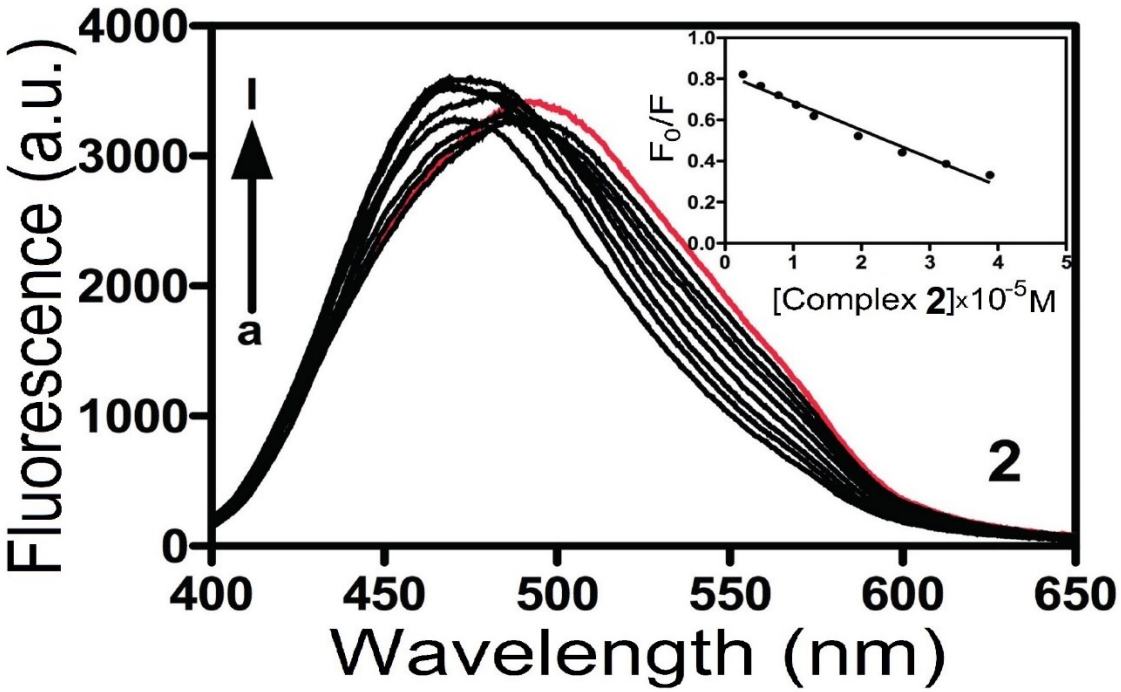
Fluorescence (a.u.)
Wavelength (nm)
I
a
2
F_0/F
[Complex 2]×10^{-5}M

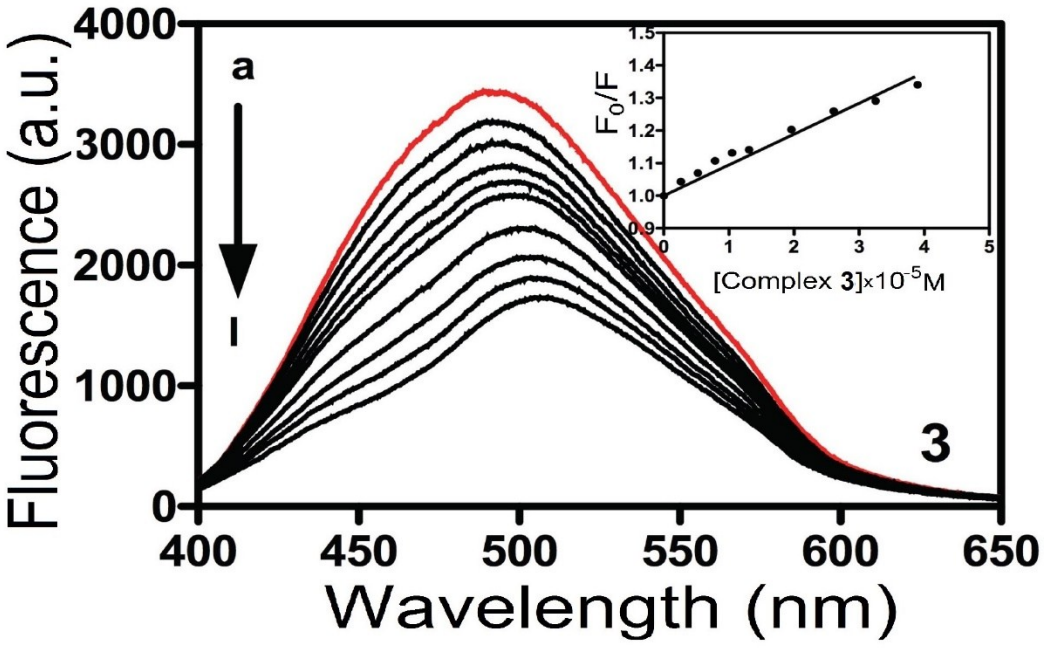
Fluorescence (a.u.)
Wavelength (nm)
a
I
3
F_0/F
[Complex 3]×10^{-5}M

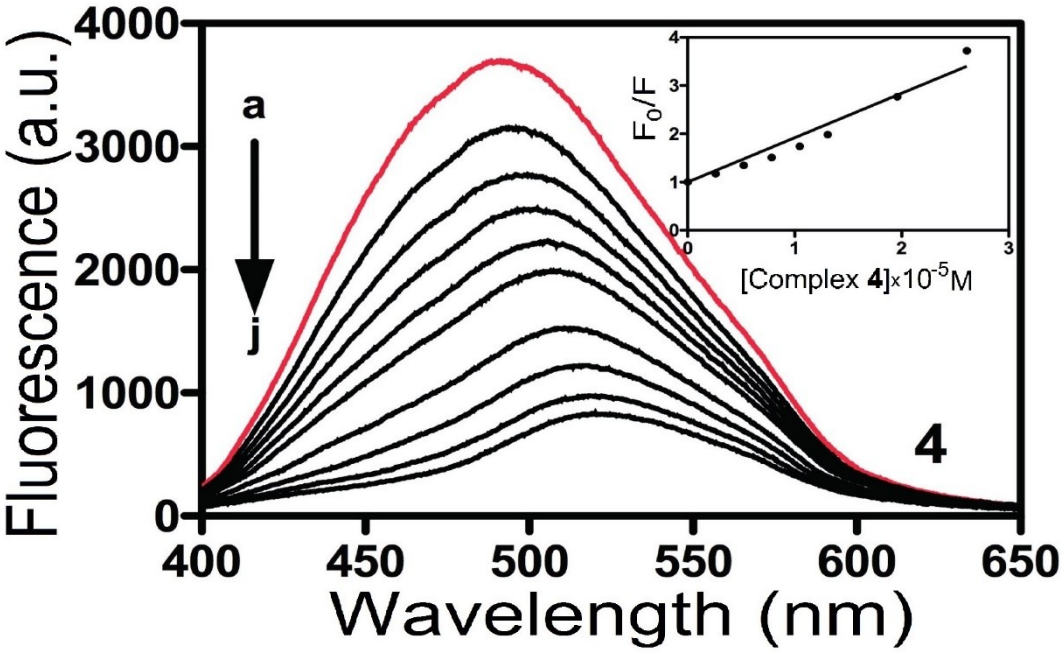
Fluorescence (a.u.)
Wavelength (nm)
a
j
4
F_0/F
[Complex 4]×10^{-5}M

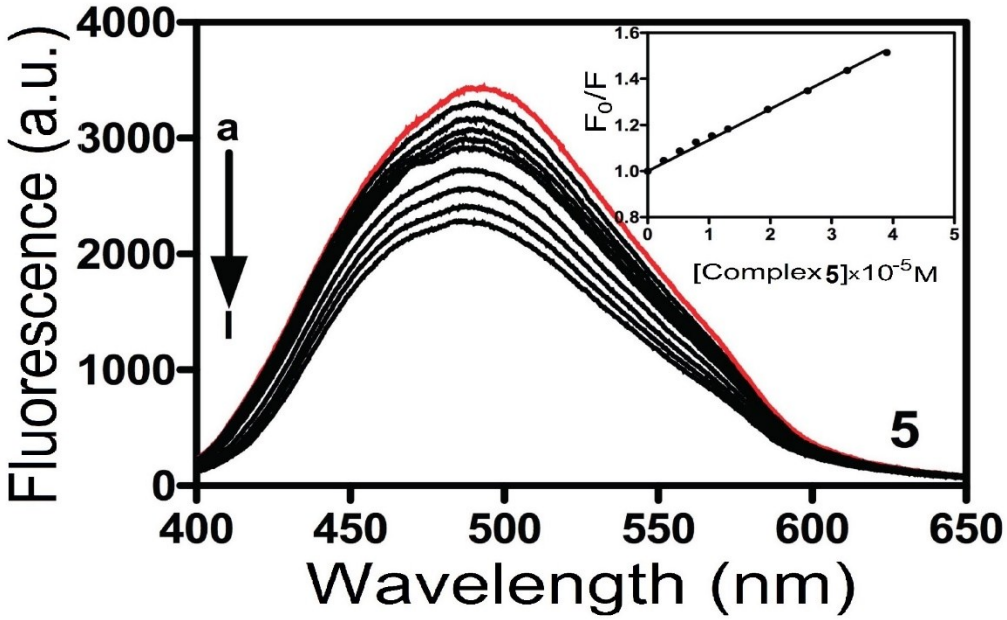
Fluorescence (a.u.)
Wavelength (nm)
a
l
5
F_0/F
[Complex 5]×10^{-5}M

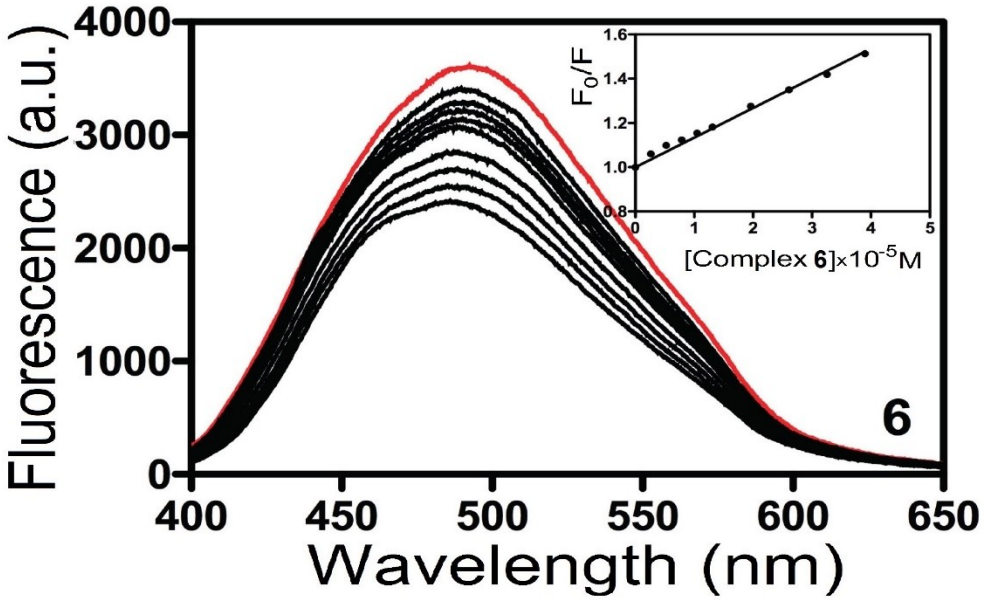
Fluorescence (a.u.)
Wavelength (nm)
6
F_0/F
[Complex 6]×10^{-5}M

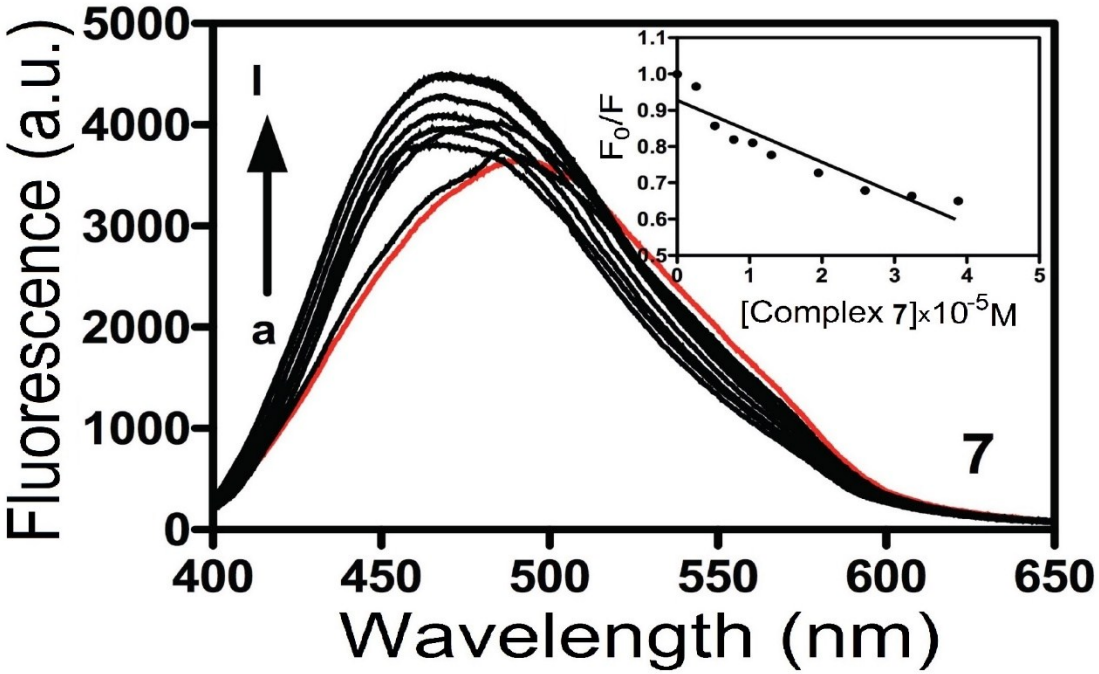
Fluorescence (a.u.)
Wavelength (nm)
I
a
7
F_0/F
[Complex 7]×10^{-5}M

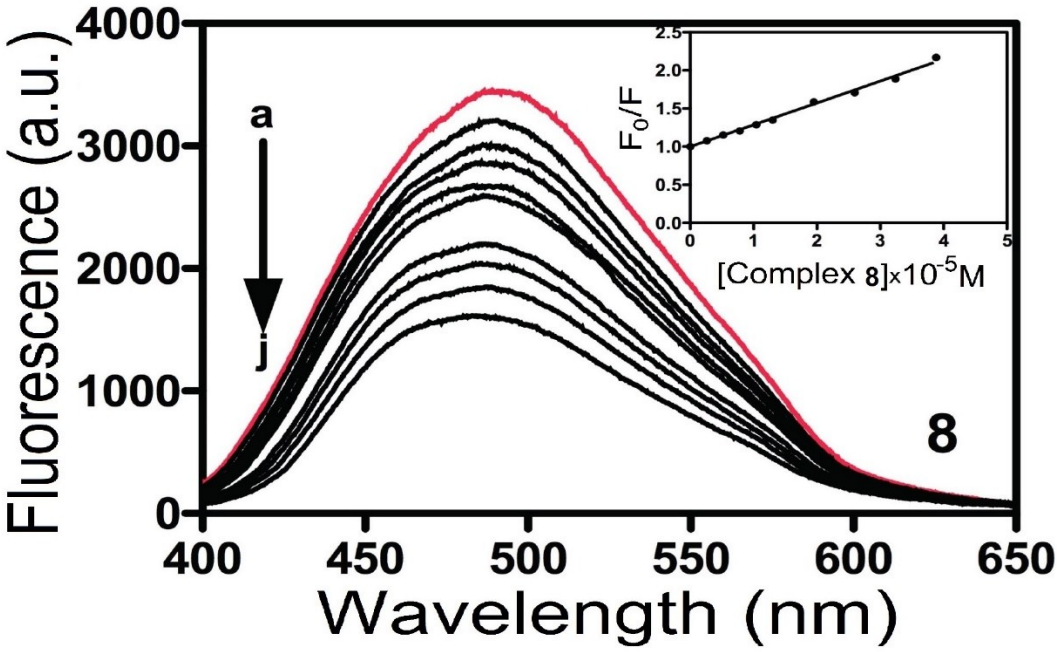
Fluorescence (a.u.)
Wavelength (nm)
a
j
8
F_0/F
[Complex 8]×10^{-5}M

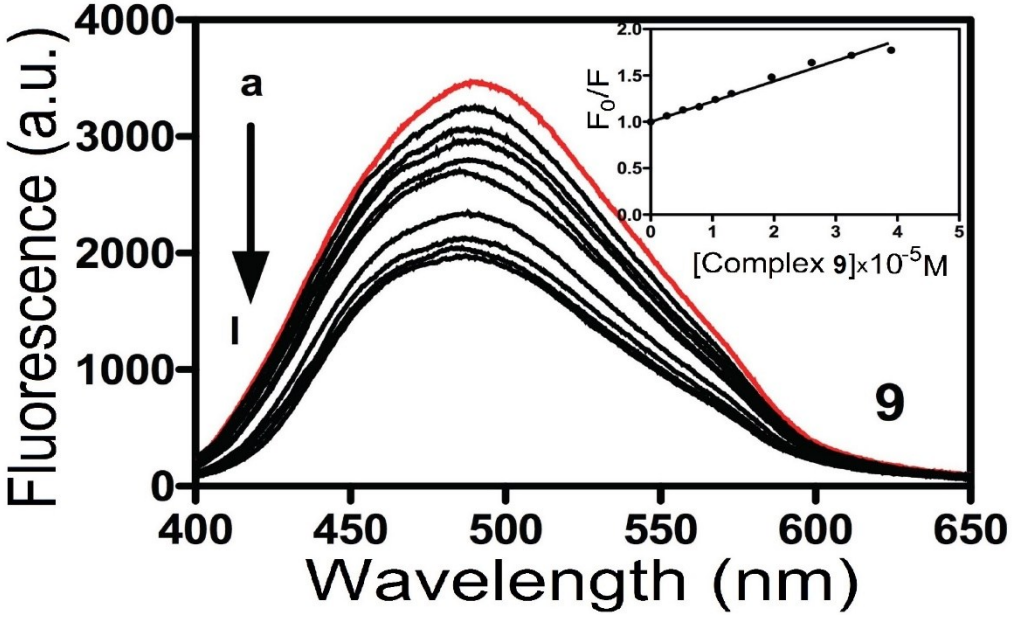
Fluorescence (a.u.)
Wavelength (nm)
a
I
9
F_0/F
[Complex 9]×10^{-5}M

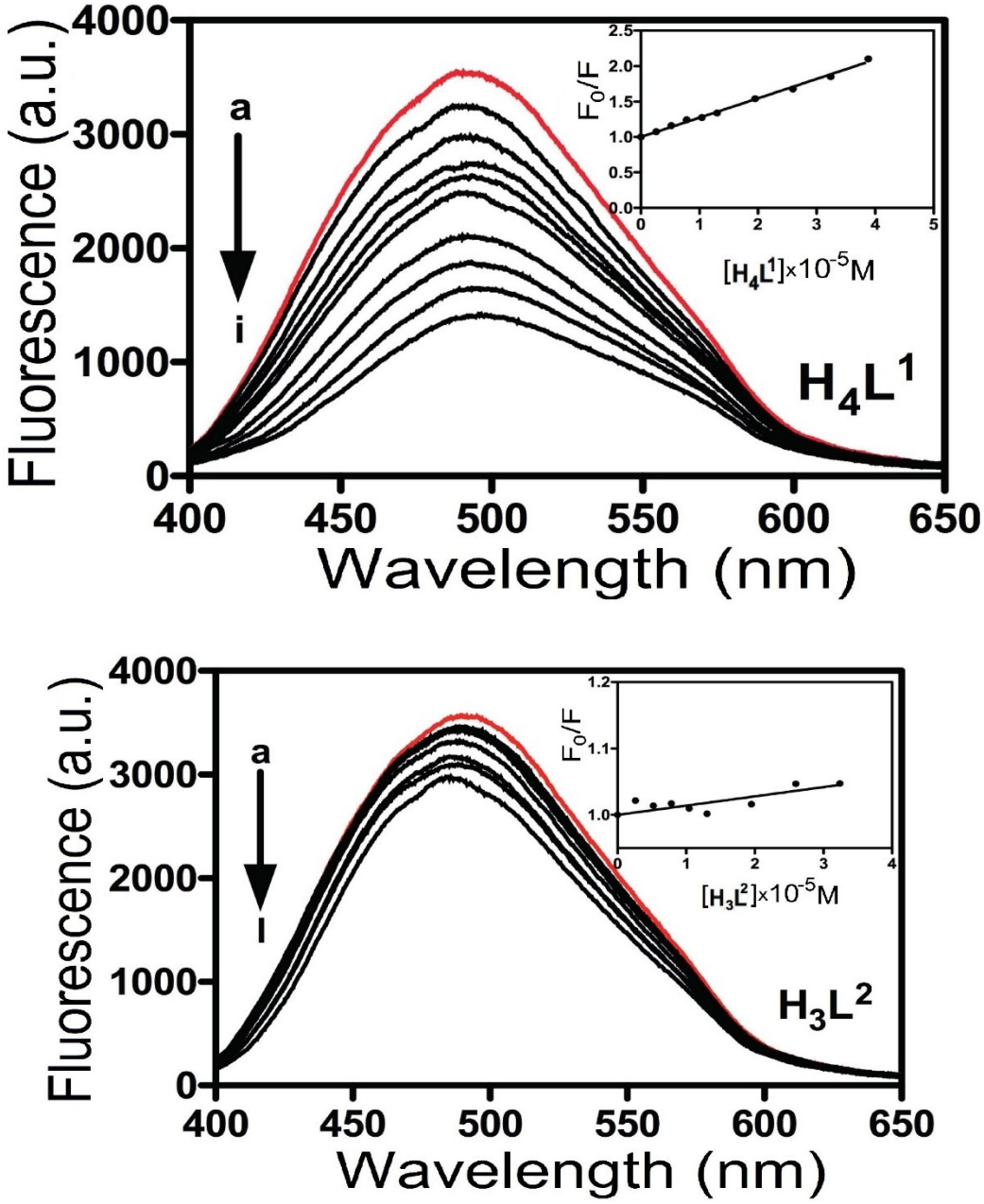

Figure 24S. Emission fluorescence spectra of DAPI-ct-DNA complex upon excitation at 338 nm in the presence of increasing concentration of different compounds and proligands in the range 0-36 μM. Experiments were performed in 10 mM phosphate buffer, pH 7.2. Inset: Stern-Volmer plot of $\mathbf{F_0/F}$ *vs.* [complex] for the titration of the complexes to DAPI-ct-DNA complex

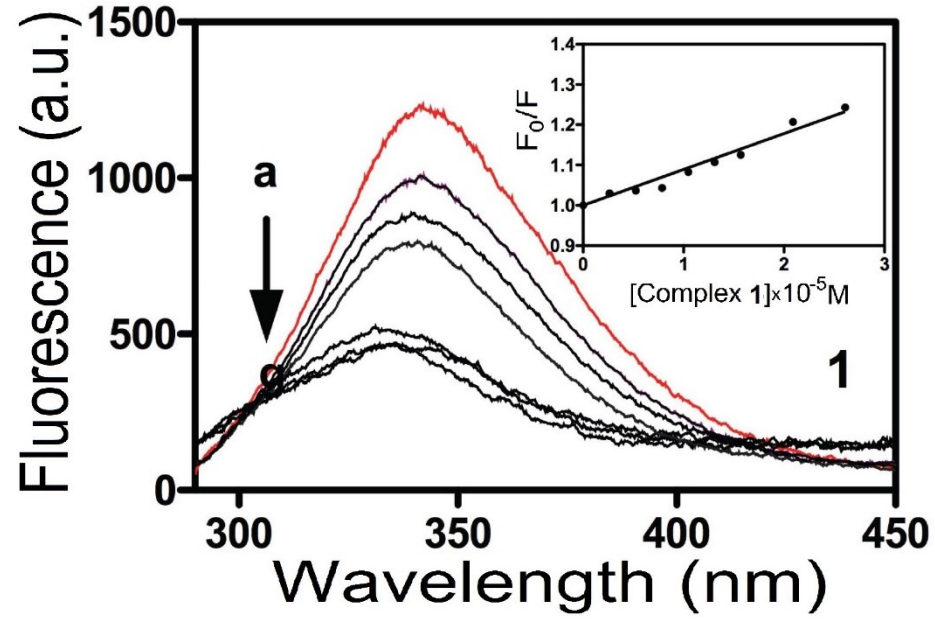
Fluorescence (a.u.)
1500
1000
500
0
a
c
300
350
400
450
Wavelength (nm)
F_0/F
1.4
1.3
1.2
1.1
1.0
0.9
0
1
2
3
[Complex 1]×10^{-5}M
1

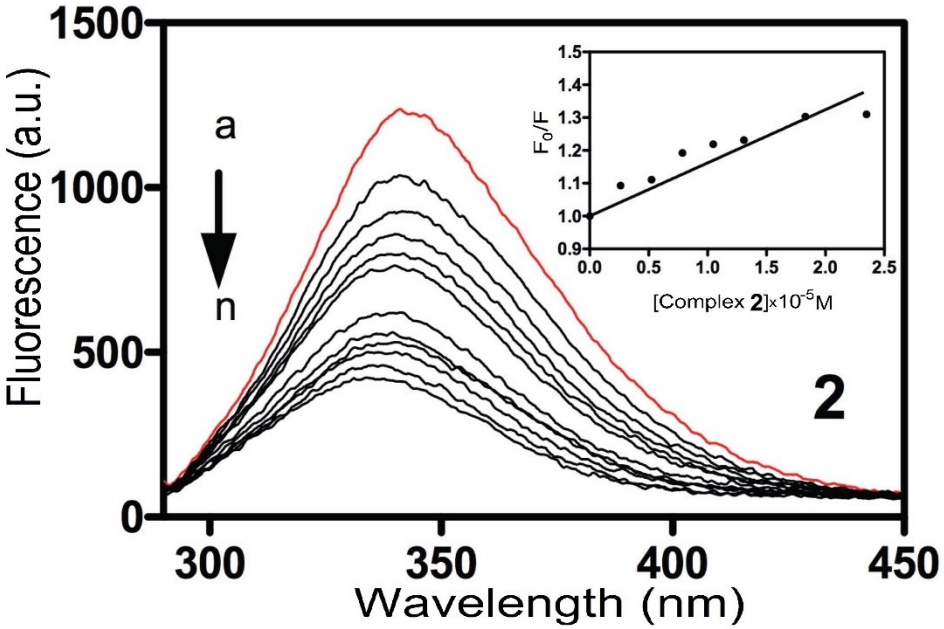
Fluorescence (a.u.)
1500
1000
500
0
a
n
300
350
400
450
Wavelength (nm)
F_0/F
1.5
1.4
1.3
1.2
1.1
1.0
0.9
0.0
0.5
1.0
1.5
2.0
2.5
[Complex 2]×10^{-5}M
2

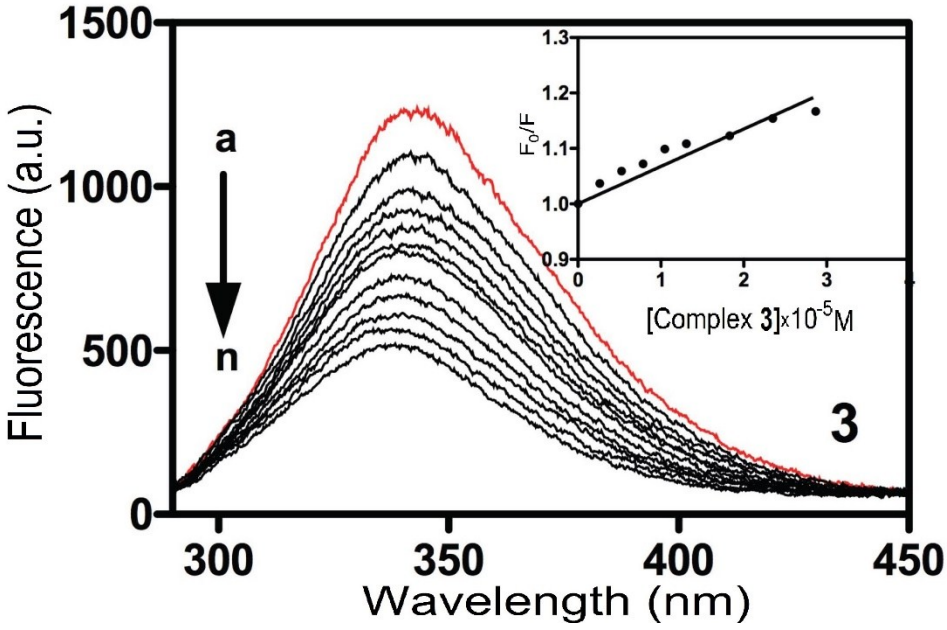
Fluorescence (a.u.)
1500
1000
500
0
a
n
300
350
400
450
Wavelength (nm)
F_0/F
1.3
1.2
1.1
1.0
0.9
0
1
2
3
[Complex 3]×10^{-5}M
3

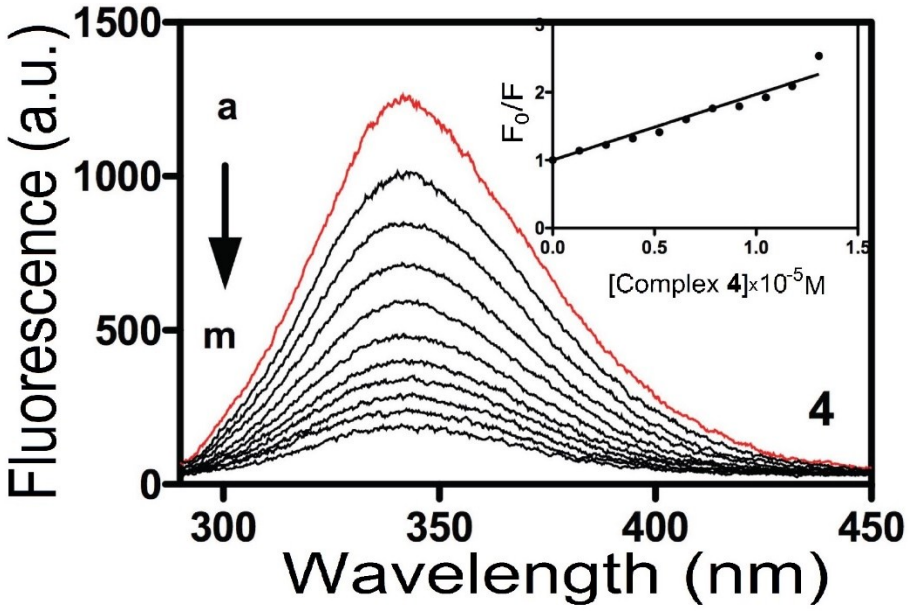
Fluorescence (a.u.)
1500
1000
500
0
a
m
300
350
400
450
Wavelength (nm)
F_0/F
[Complex 4]×10^{-5}M
4

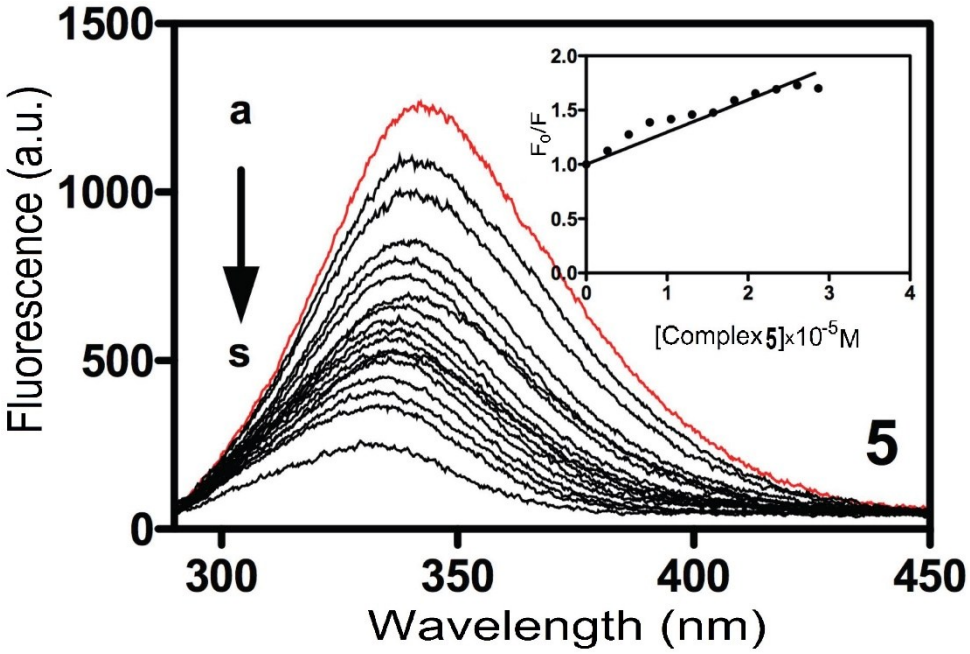
Fluorescence (a.u.)
1500
1000
500
0
a
s
300
350
400
450
Wavelength (nm)
F_0/F
[Complex 5]×10^{-5}M
5

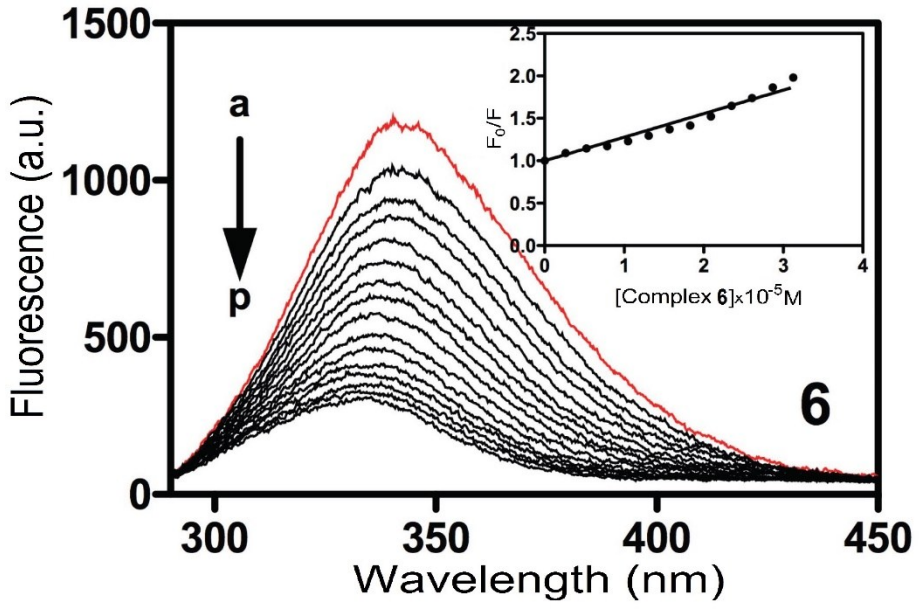
Fluorescence (a.u.)
1500
1000
500
0
a
p
300
350
400
450
Wavelength (nm)
F_0/F
[Complex 6]×10^{-5}M
6

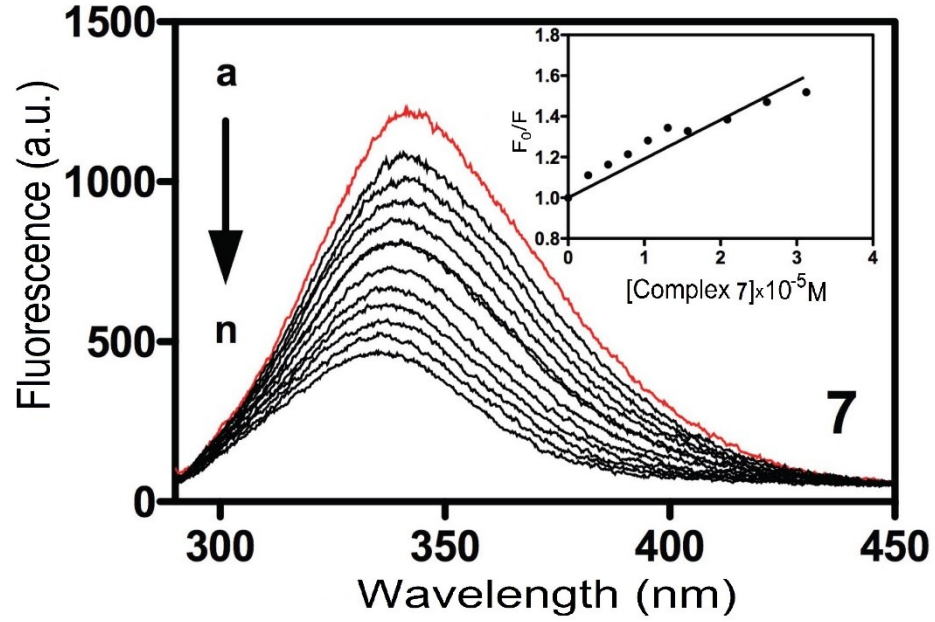
Fluorescence (a.u.)
Wavelength (nm)
a
n
7
F_0/F
[Complex 7]×10^{-5}M

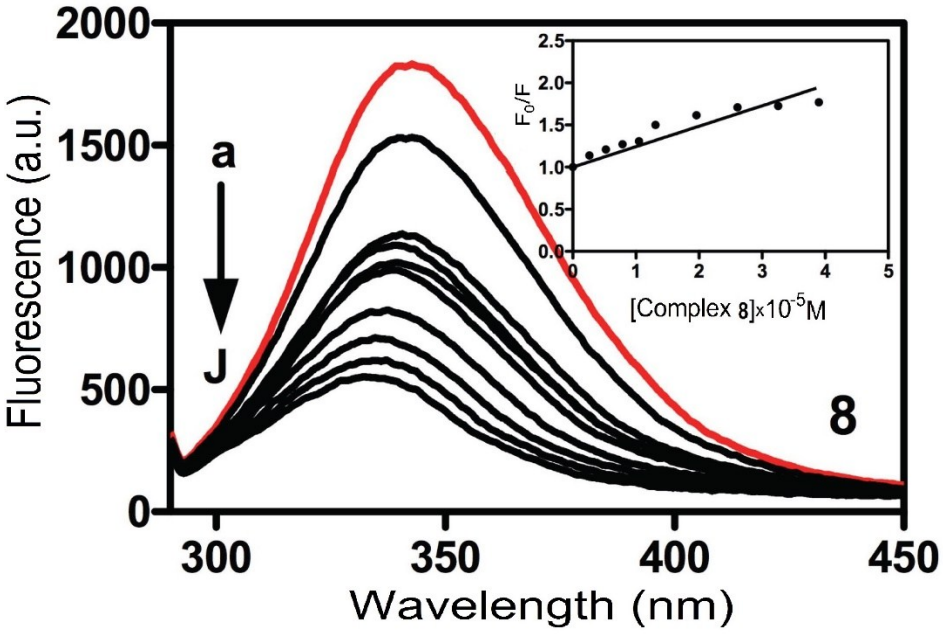
Fluorescence (a.u.)
Wavelength (nm)
a
J
8
F_0/F
[Complex 8]×10^{-5}M

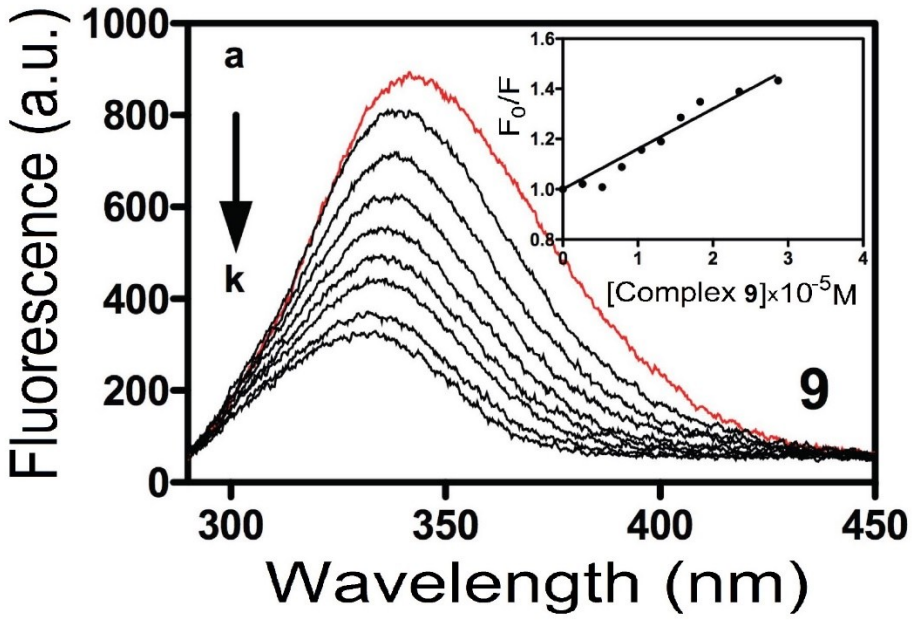
Fluorescence (a.u.)
Wavelength (nm)
a
k
9
F_0/F
[Complex 9]×10^{-5}M

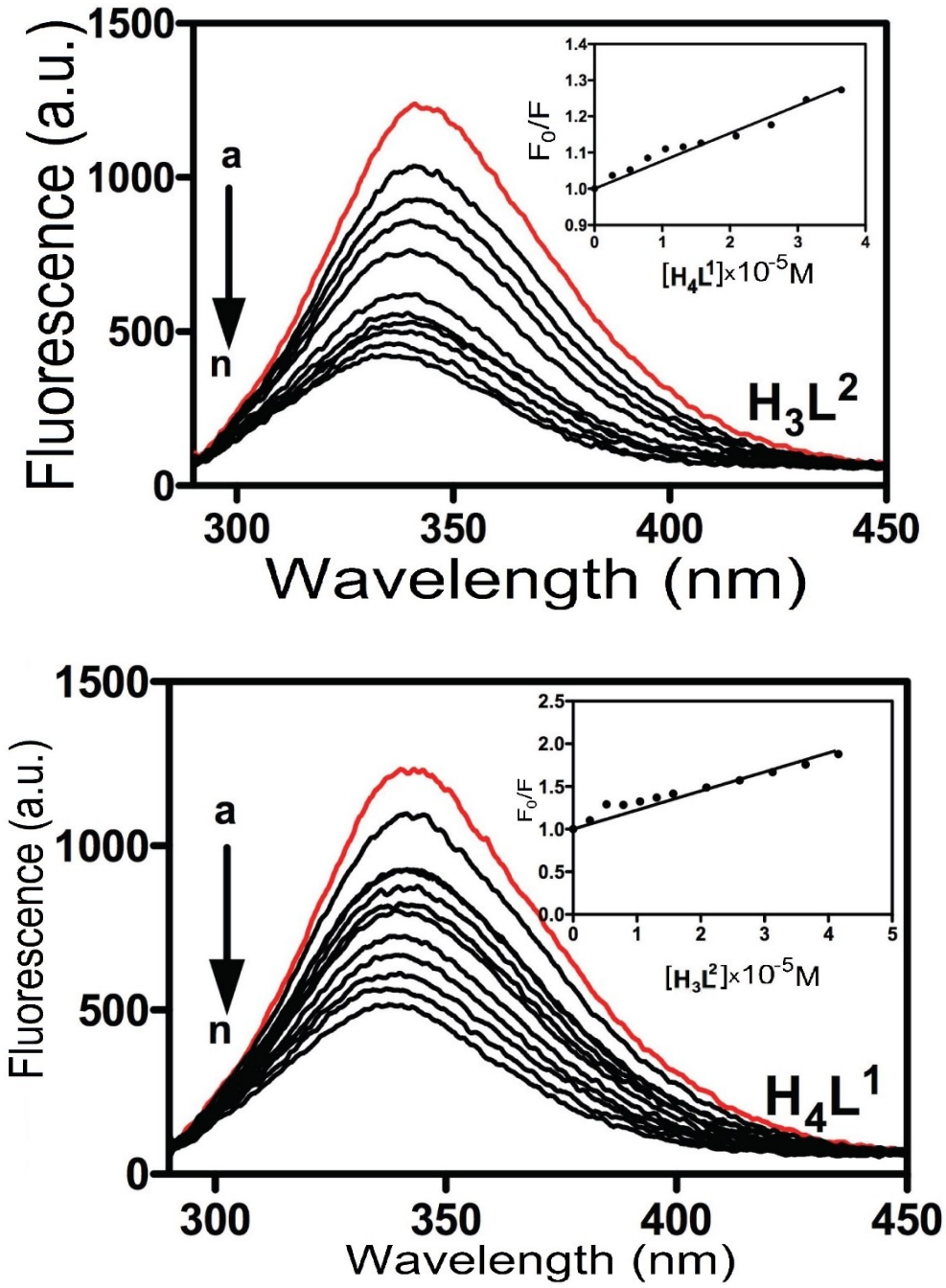

Figure 25S. Fluorescence emission spectra of BSA upon excitation at 280 nm, in the absence and presence of different concentrations of compounds and proligands. Inset, Stern-Volmer plots of $\mathbf{F_0/F}$ vs. [complex **4**] for the titration of the complexes to BSA.